Mariana Isabel Lopes Joaquim

Licenciada em Biologia

Exploring cell reprogramming techniques for Angelman Syndrome disease modelling

Dissertação para obtenção do Grau de Mestre em

Genética Molecular e Biomedicina

Orientador: Doutor Simão Teixeira da Rocha, FCT Investigator, Instituto de Medicina Molecular

FACULDADE DE CIÊNCIAS E TECNOLOGIA
UNIVERSIDADE NOVA DE LISBOA

Setembro de 2017

Exploring cell reprogramming techniques for Angelman Syndrome disease modelling

Agradecimentos

Em primeiro lugar quero agradecer ao meu orientador, Dr. Simão Teixeira da Rocha, por todo o conhecimento que me transmitiu, por toda a paciência, pelo apoio incansável e por acreditar em mim e nas minhas capacidades desde início. Este ano sob a sua orientação foi, sem dúvida, um privilégio, quer a nível profissional, quer a nível pessoal.

De seguida, agradeço à Professora Maria Carmo-Fonseca, chefe do laboratório *RNA & Gene Regulation*, por me ter aceite no seu grupo, permitindo-me desenvolver este trabalho.

Gostaria de agradecer a todos os colaboradores deste projecto: à Dra. Sofia Duarte (IMM/Centro Hospitalar de Lisboa Central) por possibilitar o acesso a pacientes com Síndrome de Angelman; ao Jerome Mertens (Salk Institute, San Diego, USA) pelo envio dos plasmídeos essenciais ao desenvolvimento de parte deste trabalho, bem como pelo contacto estabelecido connosco de forma a esclarecer quaisquer dúvidas acerca do protocolo fruto do seu trabalho; à Teresa Silva (IMM/Lisboa) e à Dra. Cláudia Gaspar (IMM/Lisboa) pelos neurónios derivados de iPSCs que constituíram um controlo importante em parte deste trabalho; ao Dr. Edgar Gomes pelo plasmídeo GFP, também ele utilizado para um controlo essencial.

A todos os meus colegas de laboratório e de gabinete, um grande obrigado. Agradeço por toda a ajuda em momentos de stress laboratorial, pelos momentos de distracção e gargalhadas e por toda a companhia ao longo deste ano. Queria agradecer especialmente ao Duarte Brandão, não só por me acompanhar em grande parte do meu trabalho mas pela inestimável ajuda dada e dúvidas tiradas. Outro agradecimento especial à Ana Raposo, por ser a minha inigualável companheira de laboratório, por todas as vezes que me ajudou em momentos de apuros e, especialmente, por me fazer rir todos os dias. Um agradecimento também à Vanessa Pires por me ter acolhido tão bem e por me ter aturado "verdinha" e ao João von Gilsa pelas gargalhadas e inigualáveis cantorias.

A todos os meus restantes amigos, um enorme agradecimento, não só pelos momentos de distracção, mas também pelo apoio moral (mesmo quando não entendem nada do que estou a dizer) e por tolerarem as minhas ausências, especialmente durante a realização deste trabalho.

Ao Duarte Próspero, pela enorme paciência, pelo carinho incomparável, pelo apoio e pelo contínuo interesse no meu trabalho e no meu futuro.

Um agradecimento enorme a toda a minha família, que sempre acreditou e continua a acreditar em mim e, em especial, um obrigado aos meus tios Jorge e São e ao meu primo Rui, sem os quais este meu percurso no ensino superior não teria sido possível.

Por fim, agradeço aos maiores impulsionadores de tudo o que se relaciona com a minha vida, os meus pais e a minha irmã, que são, sem dúvida, quem de mais perto segue os meus "sabores e dissabores" daquilo que escolhi fazer e cujo amor é incondicional.

Resumo

A Síndrome de Angelman (SA) é uma doença incurável do neuro-desenvolvimento causada pela ausência de expressão do gene *UBE3A* materno em neurónios. O *UBE3A* paterno é silenciado pelo transcrito *antisense* do *UBE3A* (*UBE3A-ATS*). No modelo de ratinho, a inibição da transcrição do *UBE3A-ATS* reactiva o *UBE3A* paterno e melhora funções cognitivas. Para avaliar se a mesma abordagem pode ser aplicada em pacientes com SA é necessário desenvolver um modelo celular desta doença.

Neste estudo visámos desenvolver esse modelo celular humano a partir de fibroblastos derivados de pacientes e avaliar o seu estado de *imprinting*.

Inicialmente foi tentado um protocolo de conversão neuronal directa baseado na expressão de dois factores de transcrição neuronais – *ASCL1*, *NGN2* – e inibidores da via SMAD de forma a converter fibroblastos em neurónios. Apesar da elevada eficiência de infecção e detecção de expressão do *ASCL1* transgénico, os iNs gerados não demonstraram sinais de identidade neuronal, baseado em resultados de RT-qPCR e IF. Este insucesso pode dever-se à falta de concentração dos lentivírus por ultracentrifugação, à falta de selecção com antibióticos e/ou ao destacamento das células durante a conversão. Seguidamente tentámos gerar NPCs a partir de iPSCs usando um protocolo comercial. No entanto, as "NPCs" geradas não expressavam os marcadores genéticos correctos. Este insucesso pode dever-se à taxa de divisão inapropriada destas células durante a indução ou à falta de pluripotência destas iPSCs.

Apesar do insucesso na geração de neurónios, conseguimos optimizar a técnica *nascent-transcript* RNA FISH, combinando a visualização do *UBE3A* com o *SNORD116*, unicamente expresso pelo alelo paterno. Esta é uma ferramenta crucial para confirmar o estado de *imprinting* do locus de Angelman nas células geradas.

No futuro, o estabelecimento de um modelo celular da SA servirá como uma plataforma de triagem de drogas para testar a reactivação do *UBE3A* paterno como alvo terapêutico para a SA.

Palavras-chave: Síndrome de Angelman, modelação de doenças, *UBE3A*, *UBE3A-ATS*, conversão neuronal directa, diferenciação neuronal de iPSCs.

Abstract

Angelman Syndrome (AS) is an imprinted neurodevelopmental disease with no cure caused by the lack of *UBE3A* expression, which, in neurons, is exclusively maternally expressed. The paternal *UBE3A* allele is silenced by the *UBE3A* antisense transcript (*UBE3A-ATS*), which is only expressed from the paternal chromosome. In AS mouse model, inhibition of the *UBE3A-ATS* transcription can reactivate paternal *UBE3A*. To translate such an approach to humans, the development of a cellular model for this disease is necessary.

Here we sought to develop cellular model systems of AS from patient-derived fibroblasts and evaluate their imprinting status using RNA FISH-based single-cell approaches.

First, a neural direct conversion protocol based on expression of two neuronal transcription factors - *ASCL1*, *NGN2* – and SMAD pathway inhibitors was tried in order to convert fibroblasts into neurons. Despite high infection efficiency and detection of transgenic *ASCL1* expression, the generated “iNs” did not show signs of neuronal identity based on RT-qPCR and IF analysis. This failure might have been caused by lack of lentiviruses concentration by ultracentrifugation, antibiotic selection skipping and/or dislodging of the cells under conversion. Second, we tried to generate NPCs from iPSCs using a commercially available differentiation protocol. Based on RT-qPCR and IF analysis, the generated “NPCs” failed to express the correct genetic markers. This failure might be explained by inappropriate accelerated division rate of the cells during induction or lack of pluripotency of the newly-generated iPSCs used.

Despite unsuccessful generation of neuronal cells, we were able to optimize nascent-transcript RNA FISH, combining *UBE3A* and paternally expressed *SNORD116*, which is a crucial tool to confirm the imprinting status of the Angelman locus in newly-generated cells.

With future efforts, the establishment of AS cellular model systems will serve as drug screening platform to test paternal *UBE3A* reactivation as a therapeutic target for AS.

Key-words: Angelman Syndrome, disease modelling, *UBE3A*, *UBE3A-ATS*, neural direct conversion, iPSCs neural differentiation.

Table of Contents

List of Figures

List of Tables

Abbreviations

AS - Angelman Syndrome

BDNF – Brain-derived neurotrophic factor

DAPI - 4',6-diamidino-2-phenylindole

DMEM – Dulbecco's modified Eagle medium

DMR – Differentially methylated region

DMSO - Dimethyl sulfoxide

DNA – Deoxyribonucleic acid

EtOH – Ethanol

FBS - Fetal bovine serum

GDNF – Glial cell line-derived neurotrophic factor

GFP – Green fluorescent protein

ICR – Imprinting control region

iPSCs – Induced pluripotent stem cells

iNs - Induced neurons

lncRNA – Long non-coding RNA

mASO – modified anti-sense oligonucleotide

NC - Neural conversion

NEAA - Non-essencial aminoacids

NM - Neural maturation

NPCs – Neural progenitor cells

PBS - Phosphate buffered saline

Pen/Strep - Penincilin/Streptomicin

PFA – Paraformaldehyde

PWS – Prader-Willy Syndrome

snoRNA – Small nucleolar RNA

SSC - Saline-sodium citrate

RNA – Ribonucleic acid

1. Introduction

1.1. Epigenetics

Epigenetics is classically defined as the field of research that studies mitotically and/or meiotically heritable changes in gene activity that does not involve alterations in DNA sequence (Sadakierska-Chudy *et al*, 2014). More recently, the concept of epigenetics has broaden and could be defined as the study of "both heritable changes in gene activity and expression and also stable, long-term alterations in the transcriptional potential of a cell that are not necessarily heritable" (Overview of the Roadmap Epigenomics Project)

Mechanistically, epigenetic regulation operates at several different levels: DNA, RNA, histones and nucleosomes. More specifically, epigenetic marks are sustained through chemical modifications at the level of DNA (e.g. methylation of cytosines at CpG sites) and post-transcriptional modifications of histones (methylation, acetylation, etc), RNA-associated silencing and remodelling of the nucleosomes (Egger *et al*, 2004; Rajender *et al*, 2011; Sadakierska-Chudy *et al*, 2014). Among the several epigenetic modifications, DNA methylation is one of the best studied cases. DNA methylation is a stable, persistent and heritable mark and influences gene expression not only by impeding binding of transcription factors but also by attracting specific methyl-binding proteins or by affecting the interaction between histone and DNA (Sadakierska-Chudy *et al*, 2014). It is regulated by both DNA methyltransferases and demethylases. DNA methyltransferases are responsible for methylation by adding methyl groups to 5' position of cytosine residues of CpG dinucleotides (reviewed in Rajender *et al*, 2011), whereas demethylases like ten-eleven translocation (TET) enzymes are responsible for converting 5-methylcytosines to 5-hydroxymethylcytosines, therefore, demethylating DNA (reviewed in Kalish *et al*, 2014).

Many biological systems such as genomic imprinting, X-chromosome inactivation, heterochromatinization and transcriptional regulation are dependent on epigenetic machinery (Sadakierska-Chudy *et al*, 2014). Disruption of this machinery can lead to incorrect expression or silencing of genes, resulting in the so-called epigenetic diseases (Egger *et al*, 2004). For example, mutations in the *DNMT3b* gene causes ICF (immunodeficiency, centromeric region instability and facial anomalies) syndrome while an expansion and inappropriate methylation of a CGG repeat in the FMR1 5' region leads to X-Fragile syndrome (Egger *et al*, 2004). It is currently known that these changes are potentially reversible and, therefore, epigenetic modifications are being explored as therapy targets for several diseases (Sadakierska-Chudy *et al*, 2014).

1.1.1. Genomic Imprinting

Genomic imprinting (imprinting for short) is an epigenetic phenomenon leading to the differential marking of genes according to their parental origin, resulting in the expression of a single parental allele (Bartolomei and Ferguson-Smith, 2011). These differential marks at the level of DNA methylation, named imprints, are established during gametogenesis and are remarkably stable throughout life (Reik and Walter, 2001). As depicted in Fig. 1.1, imprints are resistant to the major

wave of epigenetic reprogramming into a pluripotent state after fertilization, characterized by the removal of several epigenetic marks such as DNA methylation and chromatin modification, followed by *de novo* genomic methylation after embryo implantation (Bartolomei and Ferguson-Smith, 2011; Morgan *et al*, 2005). Although resistant to the epigenetic reprogramming after fertilization, in the germline of the new organism, imprints are erased at an early stage and re-established at a later stage of germ cell development according to the sex of the contributing parent for the next generation (Reik and Walter, 2001; Soellner et al, 2017).

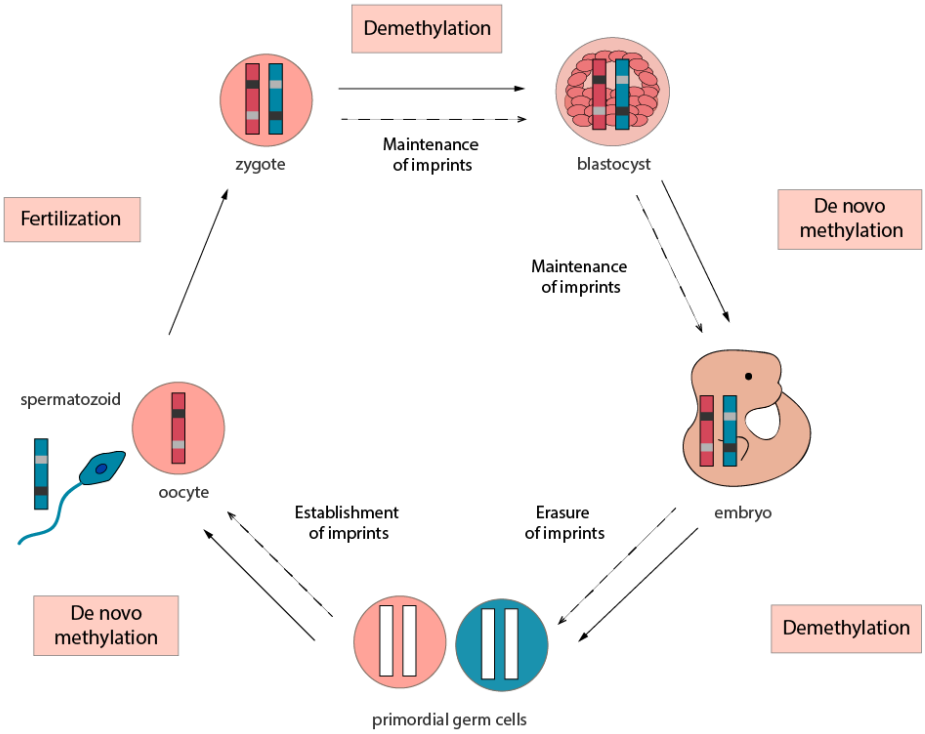

Fig. 1.1 – Representative scheme of the cycle of mammalian methylation and imprinting.

Most imprinted genes are present in clusters that are about 1Mb in length and contain both maternally and paternally expressed genes (Kalish *et al*, 2014). The imprinting of these clusters is under the control of short DNA elements named Imprinting Control Regions (ICR). ICR are typically differentially methylated regions (DMR) in which DNA is inherited from one parental germline but not from the other (Bartolomei and Ferguson-Smith, 2011; Kalish *et al*, 2014). Interestingly, there are typically long noncoding RNAs (lncRNA) in these clusters, some of which are believed to regulate the imprinting of nearby genes (Kalish *et al*, 2014). An example is the Angelman Syndrome 15q11-q13 imprinted cluster that is presented of Fig. 1.2.

Imprinting has a significant biological consequence since correct mammalian development requires genetic contributions from both maternal and paternal genomes. This was first uncovered when experimental manipulation using mouse nuclear transfer was independently performed by MacGrath and Solter and Surani *et al*, in 1984. These experiments showed that embryos reconstructed from two maternal pronuclei or two paternal pronuclei failed to survive (McGrath and Solter, 1984; Surani *et al*, 1984). Imprinted genes have been implicated in several processes such as

prenatal growth control, brain function and resource acquisition (Charalambous *et al*, 2007; Kalish *et al*, 2014). Many of these genes appear to be dosage sensitive and, therefore, functional consequences arise from changes in their expression levels (Bartolomei and Ferguson-Smith, 2011). Indeed, deletions or mutations in these genes lead to imprinted disorders. There are a group of currently 12 congenital imprinted diseases with similar underlying epi- and genetic etiologies and overlapping clinical features affecting mainly growth, development and metabolism (Soellner *et al*, 2017) (Table 1.1). For example, failure to express the paternal allele or maternal allele of genes within the *SNRPN* imprinted domain results in Prader-Willi Syndrome (PWS) and Angelman Syndrome (AS), respectively (Kalish *et al*, 2014).

Table 1.1- Summary of the 12 imprinted disorders with the affected chromosome region and main clinical features. Adapted from Bartolomei and Ferguson-Smith (2011) and Soellner *et al* (2017).

Disorder	Chromosome region	Clinical features
Transient Neonatal Diabetes Mellitus	6q24	Growth retardation, hyperglycemia, diabetes type 2 later in life.
Silver-Russel Syndrome	7p11.2-p13 and 11p15.5	Growth retardation, macrocephaly, asymmetry, feeding difficulties.
Birk-Barel mental retardation	8q24.3	Intellectual disability, hyperactivity, feeding difficulties, hypotonia.
Beckwith-Wiedemann Syndrome	11p15.5	Overgrowth, neonatal hypoglycemia, macroglossia, hemihypertrophy, increased tumor risk.
Temple Syndrome	14q32	Growth retardation, hypotonia, feeding difficulties in infancy, truncal obesity, scoliosis, precocious puberty.
Kagami-Ogata Syndrome	14q32	Growth retardation, mental retardation, placentomegaly, polyhydramnios.
Angelman Syndrome	15q11-q13	Mental retardation, speech impairment, ataxia, seizure, microcephaly, unmotivated laughing.
Prader-Willi Syndrome	15q11-q13	Mental retardation, neonatal hypotonia, obesity, hypogonadism.
Precocious puberty	15q11.2	Precocious puberty (girls 5.75 years, boys: 8.10 years)
Schaaf-Yong Syndrome	15q11.2	Hypotonia, feeding dificulties, hyperphagia, developmental delay, hypogonadism.
Sporadic Pseudo-hypoparathyreoidism 1b	20q13	Resistance to parathyroid hormone, hypocalcaemia, hyperphophatemia, abnormal growth.
Upd(20)mat	20	Growth retardation, failure to thrive.

1.2. Angelman Syndrome

Angelman Syndrome is a neurodevelopmental disorder characterized by four cardinal features: severe developmental delay, profound speech impairment, movement and balance disorder and easily excitable personality with an inappropriately happy affect (Lossie *et al*, 2001). AS is caused by disruption of the maternally expressed imprinted *UBE3A* gene in the 15q11-q13 imprinted *locus* in neurons (Margolis *et al*, 2015).

1.2.1. Symptoms

Angelman Syndrome was first described in 1965 by the English paediatrician Harry Angelman. He described three patients who presented a stiff, jerky gait, absence of speech, excessive laughter and seizures, referring to them as “puppet children” (Angelman, 1965; Margolis *et al*, 2015). This disease presents a prevalence ranging from 1 in 12000 to 1 in 20000 (Buiting *et al*, 2016) and it is characterized by developmental delay, intellectual disability, absent speech, seizures, ataxic gait, easily excitable happy demeanor iniciated by social interaction and characteristic facies (reviewed in Kalsner and Chamberlain, 2016). Usually, infants with AS do not show any signs of the disease at birth, however delayed acquirement of motor skills, language and social skills are evident within the first year of life (Bird, 2014). The clinical problems associated with AS that develop in childhood persist into adulthood, hence adults with this condition are not capable of independent living, although many can perform tasks with supervision (Kalsner and Chamberlain, 2016; Buiting *et al*, 2016). The average life expectancy of AS patients is reasonably long excepting some early deaths due to severe seizures or accidental events (Buiting *et al*, 2016).

1.2.2. *UBE3A* and the 15q11-q13 imprinted cluster

E3A ubiquitin ligase gene (*UBE3A*) encodes E3A protein, a member of the large family of E3 ubiquitin ligase proteins (LaSalle *et al*, 2015), ubiquitously expressed in human tissues (Condon *et al*, 2013). UBE3A is involved in the process of marking proteins for degradation, by transferring the ubiquitin from E2 ubiquitin conjugation enzymes to the substrate protein (Chamberlain, 2013). In neurons, UBE3A protein localizes in pre- and post-synaptic neuronal compartments and in both cytoplasmic and nuclear locations (Dindot *et al*, 2008). *UBE3A* is a gene of interest due to its implication in both Angelman Syndrome and Chromosome 15q11.2–q13.3 Duplication Syndrome and due to its regulation through imprinting and non-coding RNAs.

Genomic imprinting in 15q11-q13 locus is controlled by a bipartite ICR composed by two elements: (1) the Prader-Willi syndrome imprinting center (PWS-IC) that includes the major promoter and exon 1 of the *SNURF-SNRPN* gene. Within the PWS-IC lies a differentially-methylated region that is methylated on the maternally-inherited allele and unmethylated on the paternally-inherited allele; (2) the Angelman syndrome imprinting center (AS-IC), that is thought to establish the maternal imprint of the PWS-IC in the maternal germline by driving expression from the upstream exons of *SNURF-SNRPN*, (Chamberlain, 2013) (Fig. 1.2). The *SNURF-SNRPN* gene is expressed from the paternal allele and forms a bicistronic transcript that produces two proteins: SNURF and SNRPN (Gray *et al*,

1999). SNURF is a nuclear localized protein of unknown function that is encoded by the three fist exons of *SNURF-SNRPN* (Runte *et al*, 2001). *SNRPN* is a small nuclear ribonucleoprotein that functions in pre-mRNA processing and thought to be involved in alternative splicing (Chamberlain, 2013). Downstream of the *SNURF-SNRPN* locus, and spanning a region of around 600kb of DNA, there is more than 148 exons which encode for non-coding transcripts (Runte *et al*, 2001), as, for example, the IPW long non-coding RNA (lncRNA) and the small nucleolar RNAs (snoRNAs) such as *SNORD116* and *SNORD115* clusters (Sato, 2017).

In somatic cells the paternally expressed *SNURF-SNRPN* drives the expression of polycistronic transcript that is terminated at the IPW region (Chamberlain, 2013) leading to the expression of both *SNURF-SNRPN* and *SNORD116* snoRNAs cluster. However, in neurons, the transcription of this polycistronic transcript continues further, leading also to the expression of the *SNORD115* snoRNAs cluster and of a non-coding anti-sense transcript which partially overlaps with the *UBE3A* gene, known as *UBE3A* antisense transcript (*UBE3A-ATS*) (Meng *et al*, 2013). It is believed that *UBE3A-ATS*, which is expressed from the paternal allele (Rougeulle *et al*, 1998), is required for the silencing of the paternal *UBE3A* (Meng *et al*, 2013), resulting in exclusively maternal expression of *UBE3A* in these cells. Indeed, Meng *et al* showed that premature termination of murine *Ube3a-Ats* leads to unsilencing of paternal *Ube3a* in multiple brain regions (Meng *et al*, 2013). To explain this repression, Buiting *et al* proposed a transcriptional collision model where two opposing polymerases for *Ube3a* and *Ube3a-Ats* on the paternal chromosome collide into each other around intron 4 of *Ube3a*, which would provoke stalling and dissociation of both polymerases, thereby terminating the transcription of *Ube3a* and its antisense (Buiting *et al*, 2016). However, formal proof of this mechanism remains to be tested.

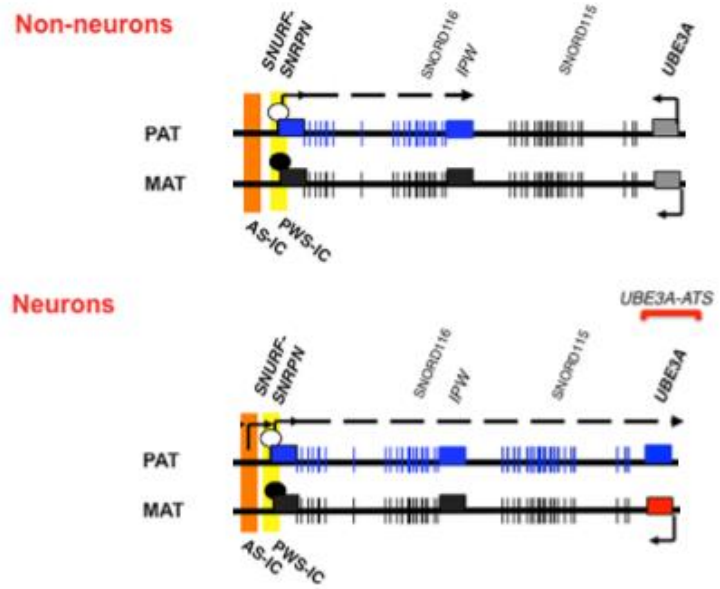

Fig. 1.2 – Map of the human 15q11-q13 imprinted region in non-neurons (top) and neurons (bottom). Blue rectangles represent imprinted transcripts that are paternally expressed; red rectangles represent imprinted transcripts that are maternally expressed; black rectangles represent imprinted transcripts that are repressed; grey rectangles represent transcripts that biallelically expressed. AS-IC corresponds to the Angelman Syndrome imprinting center and PWS-IC represents the Prader-Willi Syndrome imprinting center; the white circles represent unmethylated PWS-IC whereas the black circles represent methylated PWS-IC. Adapted from Chamberlain (2013).

1.2.3. Causes

Four molecular events can be at the origin of the maternal *UBE3A* lack of function in Angelman Syndrome: large deletions (around 5-7 Mb), also known as microdeletions, within the maternal chromosomal region 15q13-q11 (70-80%); mutation in the maternally inherited copy of *UBE3A* (10-20%); imprinting defect causing lack of expression of the maternal copy of *UBE3A* (3-5%); paternal uniparental disomy (UPD) (3-5%) (Lossie *et al*, 2001; Margolis *et al*, 2015). The diverse etiologies correlate with gradual differences in the severity of the disorder: large deletions result in loss of several other genes in the same region, therefore, patients with deletion within the maternal chromosomal region 15q13-q11 typically present a more severe phenotype than, for example, patients carrying point mutations affecting the *UBE3A* gene alone (Mertz *et al*, 2014; Stanurova *et al*, 2016).

1.2.4. Diagnosis

Angelman Syndrome can only be confirmed by molecular diagnosis, which starts with the determination of the DNA methylation status of the *SNURF-SNRPN* promoter region (Williams *et al*, 2006), since the majority of Angelman patients will be positive for this test. Indeed, absence of maternal methylation pattern secures the diagnosis of AS (Margolis *et al*, 2015). The diagnosis proceeds to unravelling the cause of the disease as depicted in Fig. 1.3. Fluorescent *in situ* hybridization searches for a deletion within 15q11-q13 region and microarray allows the determination of the deletion size (Margolis *et al*, 2015). If a deletion is not found, diagnosis proceeds to DNA marker analysis of parent's chromosome 15q11-q13 to confirm or exclude UPD. In the presence of two paternal copies, UPD is confirmed (Kalsner and Chamberlain, 2016) If both deletion and UPD are excluded, AS is probably due to an imprinting defect, caused by epigenetic phenomena or imprinting center point mutations or deletions (Margolis *et al*, 2015). For those patients with AS-related symptoms but a negative methylation test, *UBE3A* sequencing is performed and should detect a mutation within this gene. If not, AS is unlikely to be the diagnosis.

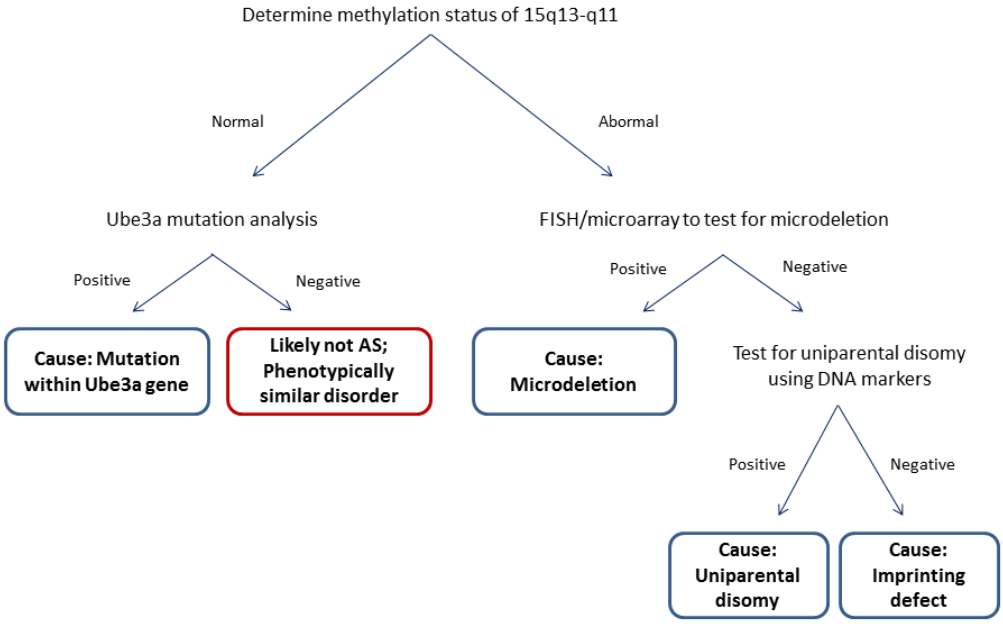

Fig. 1.3 – Representative scheme of Angelman Syndrome molecular diagnosis. Adapted from Margolis *et al* (2015).

1.2.5. Treatment

Currently there is no cure for Angelman Syndrome and the treatment for this disease is exclusively symptomatic. The management of AS requires a many-sided approach and is based on therapies that can improve the quality of patient's life (Sachdeva *et al*, 2016) targeting epilepsy, sleep disturbance, muscle tone and gait, diet, speech and others (reviewed Kalsner and Chamberlain, 2016). Usually, seizures are treated with anticonvulsants, sleep problems are approached with a combination of pharmacology and therapies to mitigate gross and fine motor delay are used. At the level of communication, alternative strategies are tried such as the use of devices, picture exchange cards and modified sign language (Margolis *et al*, 2015).

1.2.5.1. Therapeutic approaches under investigation

AS is incurable but some therapeutic approaches are currently under investigation. Since AS is caused by *UBE3A* deficiency, recent research towards therapeutic approaches have focused on methods enabling the restoration of *UBE3A* expression in the mouse model, either by direct gene therapy or by un-silencing the paternal allele (Bi *et al*, 2016).

Injection of recombinant adeno-associated virus carrying the mouse *Ube3a* into the hippocampus of AS mice was attempted by Daily *et al* in 2011. This approach restored local *Ube3a* expression and improved hippocampus-dependent learning and memory. However, *Ube3a* expression in the cerebellum was not increased and there was no effect on motor dysfunction (Daily *et al*, 2011). One concern of this approach is the control of *UBE3A* expression, since high levels of *UBE3A* constitute a risk factor for autism spectrum disorder (Bi *et al*, 2016). Since this experiment in 2011 there has been no follow-up or any advancement using this approach.

In 2012, Huang and his co-workers showed that topoisomerase inhibitors can unsilence the dormant allele of murine *Ube3a* in neurons (Huang *et al*, 2012). They developed a high-content screen using primary mouse cortical neurons from *Ube3a*-Yellow Fluorescent Protein knockin mice (Huang *et al*, 2012). They identified twelve topoisomerase I inhibitors and four topoisomerase II inhibitors that unsilenced the paternal *Ube3a* allele. Topotecan, a topoisomerase I inhibitor, was found to be the most effective, even at nanomolar concentration (Huang *et al*, 2012). It was latter shown that topotecan acts by stabilizing the formation of RNA:DNA hybrids at repeat elements within paternal *Snord116*, which leads to an increase in chromatin decondensation and inhibition of *Ube3a-Ats* expression (Powell *et al*, 2013). The inhibition of transcriptional progression of *Ube3a-Ats* leads to un-silencing of the paternal copy of *Ube3a* in AS model mice (Huang *et al*, 2012). Since topotecan is an FDA-approved anti-cancer drug, these results encouraged the study of this drug as a therapeutic approach for AS (Bi *et al*, 2016). However, in 2016, a study exploring the specificity of topotecan showed that the expression of many more genes was altered in the topotecan-treated wild-type neurons than in those neurons with topoisomerase I deletion (Mabb *et al*, 2016). These results raised the concern of topotecan unintended off-target effects (Tan and Bird, 2016).

More recently, the usage of anti-sense oligonucleotides (ASOs) became a promising novel therapeutic approach to treat AS (Meng *et al*, 2015). ASOs are synthetic single stranded oligonucleotides that target RNA for degradation: the ASO binds to the target RNA in the nucleus and

RNaseH cleaves the RNA strand of the ASO–RNA heteroduplex which results in subsequent target RNA degradation by exonucleases (Wu *et al*, 2004). Meng *et al*, in 2015, administered phosphorothioate-modified chimaeric 29-O-methoxyethyl DNA ASOs, complementary to a 113 kilobase pair region of mouse *Ube3a-Ats* downstream of the *Snord115* cluster of snoRNAs, in AS mice via intracerebroventricular injection. ASO treatment achieved not only specific reduction of *Ube3a-Ats* but also sustained unsilencing of paternal *Ube3a* in neurons (Meng *et al*, 2015). Moreover, *Snrpn*, *Snord116* and *Snord115* expression was not affected by the ASO treatment, neither by increasing dose or time of the treatment (Meng *et al*, 2015). Restoration of Ube3a protein was only partial but it was sufficient to ameliorate some cognitive deficits such as memory impairment, although motor deficits did not seem to be rescued at any level (Bi *et al*, 2016). Meng *et al* postulated that complete phenotypic reversal might require treatment before a critical developmental window, a longer recovery time or a higher *UBE3A* induction level. Actually, a study investigating the effects of reinstating *Ube3a* expression during distinct neurodevelopmental windows of mice showed that AS-relevant phenotypes are only fully rescued during a very early time window, in the embryonic stage (Silva-Santos *et al*, 2015). The reinstatement of *Ube3a* in juvenile mice rescued the motor coordination deficits, which was not seen at later stages (Silva-Santos *et al*, 2015).

In any case, the use of modified ASOs (mASOs) against *UBE3A-ATS* is a promising therapeutic approach for AS. However, whether downregulation of the *UBE3A-ATS* is achievable using mASOs in humans and in which developmental time window ameliorates AS symptoms remains to be investigated.

1.3. Cellular models of human neuronal diseases

The study of human neurological disorders and the basic mechanisms behind those diseases have been limited for a long time by the lack of human brain cells for experimental purposes (Mertens *et al*, 2016). Many studies on certain neuronal dysfunctions have been restricted to analysis of *post-mortem* tissues of patients. In addition of being poorly preserved, these tissues usually represent the end-stage of the disease (Nikoletopoulou and Tavernarakis, 2012). Although animal models, mainly mouse models, have contributed greatly to the better understanding of disease mechanisms, they do not fully recapitulate the human phenotype of the disease (Onuki and Takahashi, 2015). Also, most human neurological diseases arise from multiple factors, which are very often not represented by the model organisms (Mertens *et al*, 2016).

Recently, technologies for deriving human neurons *in vitro* have upgraded our ability to study cellular and molecular aspects of human neurons (Vadodaria *et al*, 2016). These promising technologies allow the generation of patient-specific cell lines which may serve as tools for understanding disease pathogenesis, for drug screens and, potentially, for cell replacement therapies (Pfisterer *et al*, 2011a).

We can consider two main approaches for deriving reprogrammed human neurons from patients: neuronal differentiation from somatic cell-derived induced pluripotent stem cells and direct conversion of somatic cells into induced neurons (Mertens *et al*, 2016).

1.3.1. Pluripotent stem cells

Human pluripotent stem cells (hPSCs) are normal primary cell lines with intrinsic capability for indefinite self-renewal and with the competence to, potentially, adopt any cellular fate through differentiation (Avior *et al*, 2016). hPSCs comprise human embryonic stem cells (hESCs) and induced pluripotent stem cells (iPSCs) (Mertens *et al*, 2016).

hESCs are originated from the late human blastocyst and have the unique potential to endlessly divide while maintaining an undifferentiated state and the capacity to differentiate into all germ layers as well as extra-embryonic tissues or placental cells (Menon *et al*, 2016). Because of these features, hESCs have emerged as an attractive model system to understand embryonic development and a promising source for cell-based therapies, drug studies and disease modelling (Murry and Keller, 2008). However, advances in embryonic stem cell technologies are limited by the controversial source of hESCs (Menon *et al*, 2016). Hence, the isolation of hESCs from human embryos raised serious ethical concerns, prompting efforts to find alternative sources of pluripotent cells (Sommer and Mostoslavsky, 2012). Furthermore, hESCs are not patient-specific and therefore not amenable for cell-replacing therapies due to possible immune rejection.

1.3.2. Induced pluripotent stem cells

Pluripotency can also be regained from cells of later development stages or even adult cells (Menon *et al*, 2016). The first steps in reprogramming somatic cells were given by Gurdon *et al*, in 1958, using nuclear transplantation. They showed that transplantation of the nuclei of intestinal epithelial cells from tadpoles into *Xenopus* eggs allowed the development of normal and mature tadpoles (Gurdon *et al*, 1958). Almost 50 years later, in 2006, a major step towards reprogramming was done by Takahashi and Yamanaka that demonstrated induction of pluripotent stem cells from mouse embryonic or adult fibroblasts by introducing four factors: *OCT3/4*, *SOX2*, *C-MYC* and *KLF4* (Takahashi and Yamanaka, 2006) (Fig. 1.4). The obtained cells exhibited the morphology and growth properties of ESCs and expressed ESC marker genes, besides being capable of differentiating in the three germline layers (Takahashi and Yamanaka, 2006; Takahashi *et al*, 2007). Since then, the number of iPSCs generation protocols has enormously raised and currently there are several methods available.

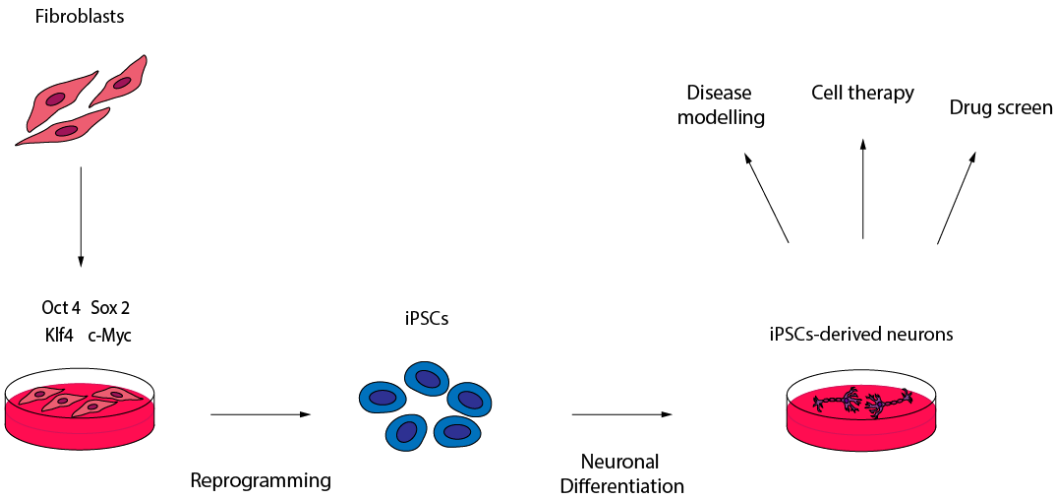

Fig. 1.4 – Representative scheme of iPSCs reprogramming and neuronal differentiation.

1.3.2.1. Reprogramming techniques

The original method for generating iPSCs used retroviral transduction to obtain expression of the four factors (Immamura and Inoue, 2012). Retroviral transduction has already been successfully used for reprogramming several cell types such as mouse and human fibroblasts, neural stem cells, keratinocytes, adipose cells, liver cells and blood cells (reviewed in Menon *et al*, 2016). In order to enhance the reprogramming efficiency, Sommer and colleagues used instead a lentiviral vector which led to a ten-fold increase of the reprogramming efficiency (Sommer *et al*, 2009). Nevertheless the use of integrating retroviruses or lentiviruses to deliver the reprogramming factors constitutes a drawback of iPSCs reprogramming since resulting iPSCs clones can display proviral integrations that increase the risk of insertional mutagenesis (Sommer and Mostoslavsky, 2012). Additionally, *C-MYC* is a known proto-oncogene that, with prolonged infection with retroviruses, may be aberrantly expressed and may induce oncogenic transformation (Immamura and Inoue, 2012; Sommer and Mostoslavsky, 2012). In any case, the use of lentivirus for iPSCs reprogramming remains the most used method in iPSCs research.

There are alternative reprogramming techniques available that circumvent the potential risks of viral approaches such as replication-defective adenoviral vectors, self-replicating episomal vectors and non-viral minicircle DNA vectors (reviewed in Menon et al, 2016). Despite being non-integrating approaches, these techniques yields very low reprogramming efficiencies.

1.3.3. iPSCs in disease modelling

iPSCs are a virtually unlimited source of autologous cells, with self-renewing capacity and plasticity (Menon *et al*, 2016). Moreover, reprogramming allows the development of disease-specific iPSCs lines that can recapitulate the human pathologic condition *in vitro* (Sommer and Mostoslavsky, 2012). This recapitulation based on the genetic material of the patient might give a reliable model of the patient's disease (Nikoletopoulou and Tavernarakis, 2012). The first report of disease models

using iPSCs occurred in 2008, when Park *et al* generated iPSCs from patients with a variety of genetic diseases with either Mendelian or complex inheritance (Park *et al*, 2008).

One drawback of iPSCs generation is that it is a very laborious and time-consuming process (Ohnuki and Takahashi, 2015.) In fact, differentiation of fibroblasts into neural cells via iPSCs reprogramming usually takes 4-6 months before functional neurons are generated (Mertens *et al*, 2016). Another core aspect of the reprogramming protocols is the importance of monitoring of the iPSCs epigenetic state. In fact, Nazor *et al* identified iPSC-specific epigenetic and transcriptional aberrations in genes linked to X chromosome inactivation and genomic imprinting, which were not corrected during differentiation (Nazor *et al*, 2012). Hiura *et al* examined the status of imprinted genes in five iPSCs lines and found abnormalities such as loss of imprinting, although at low levels (Hiura *et al*, 2013). Nevertheless, these results demonstrate that the analysis of the epigenetic status during reprogramming and differentiation is a critical safety step for iPSCs-based epigenetic disease models (Nazor *et al*, 2012 and Hiura *et al*, 2013).

1.3.3.1. iPSCs in neuronal disease modelling

The modelling of neuronal diseases can be done through the differentiation of iPSCs into specific neuronal cell types, with the first step being their differentiation into neuronal progenitor cells (NPCs) (Immamura and Inoue, 2012). NPCs, unlike iPSCs, are proliferative cells with limited capacity for self-renewal, giving origin to neuronal and glial progeny (Seaberg and van der Kooy, 2003). Neuronal differentiation of iPSCs has been efficiently achieved by using the knowledge gained from studying neurulation and the patterning of the early nervous system, namely, using neuronal inductive cues (Nikoletopoulou and Tavernarakis, 2012). The goal was to artificially recapitulate the signalling environment that the region-specific progenitors normally experience, which induces the expression of a combinatorial set of transcription factors characteristic of the desired neuronal cell type (Tamburini and Li, 2017). More specifically, the inhibition of activin, Nodal, TGF-β and bone morphogenetic protein signalling through SMAD signalling inhibitors such as Noggin, dorsomorphin and SB431542 has allowed the efficient neural induction of iPSCs (Immamura and Inoue, 2012).

The first reports of neural disease modelling occurred in 2008. Dimos *et al* generated iPSCs from an 80 years-old woman with amyotrophic lateral sclerosis and differentiated them into motor neurons (Dimos *et al*, 2008). In another study, Lee *et al* modelled Familial dysautonomia, an autosomal recessive congenital neuropathy, from reprogramming of fibroblasts from juvenile patients (Lee *et al*, 2009). More recently, studies have been developed with the aim of enhancing the efficiency of previous neural differentiation protocols and of directing the differentiation into defined types of neurons equivalent to *in vivo* cell populations (Nikoletopoulou and Tavernarakis, 2012).

Importantly, neuronal differentiation of iPSCs is well suited for modelling of neurodevelopmental disorders, such as Angelman Syndrome, since these disorders are characterized by an early-onset and reprogramming recapitulates the early steps of neuronal commitment (Nikoletopoulou and Tavernarakis, 2012).

1.3.4. Direct conversion into induced neurons

Direct conversion is a process that converts somatic cells into cells of different lineages, bypassing an intermediate pluripotent stage (Gopalakrishnan *et al*, 2017). This approach utilizes the overexpression of cell type-specific transcription factors to activate lineage changes and direct cellular identity towards the desired cell type (Mertens *et al*, 2016). Neurons can also be generated by direct conversion, being fibroblasts the most common source cells for neural direct conversion. The earliest report of direct conversion took place in 2010 when Vierbuchen *et al* identified, from a pool of nineteen, three neural-lineage specific transcription factors – *ASCL1*, *BRN2* and *MYT1L* (BAM factors) - able to convert embryonic and postnatal mouse fibroblasts into functional neurons *in vitro* (Vierbuchen *et al*, 2010). The resulting induced neurons (iNs) expressed neural-specific proteins, generated action potentials and formed functional synapses (Vierbuchen *et al*, 2010). This study provided the first proof that accessible cells like dermal fibroblasts can be converted to functional neurons (Kim *et al*, 2012). Only one year later, several laboratories reported the generation of iNs from human fibroblasts (reviwed in Mertens *et al*, 2016). The iNs generated by neural direct conversion can potentially be used for multiple applications such as disease modelling and drug screening (Fig. 1.5).

Lineage reprogramming technique represents a time-saving process, when compared to other reprogramming approaches, since iNs are obtained within two to three weeks upon transcription factor overexpression, which constitutes the major advantage of this approach (Mertens *et al*, 2016). The resulting iNs have the ability to give rise to multiple neuronal subtypes, allowing to generate neuronal cells that are affected in many different neuronal diseases (Kim *et al*, 2011). One common aspect observed among studies generating different subtypes of neurons is that the conversion occurs within a short period upon factor introduction and neuronal identity is rapidly acquired, however subsequent functional maturation takes several weeks (Kim *et al*, 2012). Lineage reprogramming of somatic cells can be successfully performed on parental cells with different ages, although iNs derived from embryonic or neonatal human cells seem to functionally and physiologically mature much faster than adult cell derived iNs (Kim *et al*, 2011). Direct conversion benefits from common advantages with iPSCs reprogramming such as development of disease-specific lines that recapitulate the pathologic human condition *in vitro* and absence of immunological response due to host derived donor cells (Kim *et al*, 2011). A very important aspect of converted neurons, regarding regenerative medicine, is that they are directly reprogrammed into the target cells, which means that *in vivo* teratoma formation should not be a problem, contrary to iPSCs-derived cells (Kwon *et al*, 2016).

A big limitation of direct conversion is the inability to expand the reprogrammed cells in sufficient quantity for the intended applications (Kim *et al*, 2012), since the source of the initial cells is limited. Another important drawback of this technique is that the reprogramming efficiency is even lower than that of iPSCs technology (Kwon *et al*, 2016). Although the current conversion efficiencies may be sufficient for *in vitro* studies, it might not represent a sufficient amount of cells for, for example, large-scale therapeutic screening, disease modelling and cellular therapy (Gopalakrishnan *et al*, 2017). However, given that this is a very recent research field, direct conversion is still mainly focused on proof-of-principle experiments rather than improving efficiency (Kown *et al*, 2016). It is also important to note that, regarding the recapitulation of developmental stages, direct conversion skips the

precursor stages and gives origin to neurons that have never been in an NPC-like stage. This can constitute a drawback in the case of modelling diseases whose phenotype is thought to develop from precursor cells (Mertens *et al*, 2016). Therefore, a useful approach that may resolve the two drawbacks referred above is direct conversion to induced neural stem/progenitor cells (iNSCs/iNPCs) since these recapitulate some stages of neurodevelopment as well as they are expandable cell lines (Kim *et al*, 2012). This has already been successfully attempted by several groups, who were able to directly convert adult human fibroblasts into expandable iNPCs (Mitchell *et al*, 2014; Meyer *et al*, 2015; Capetian *et al*, 2016). However, using this approach, the final goal, which is to obtain neurons, gets delayed since it adds one more cell-stage prior to neurons, instead of directly convert the fibroblasts into mature neuronal cells.

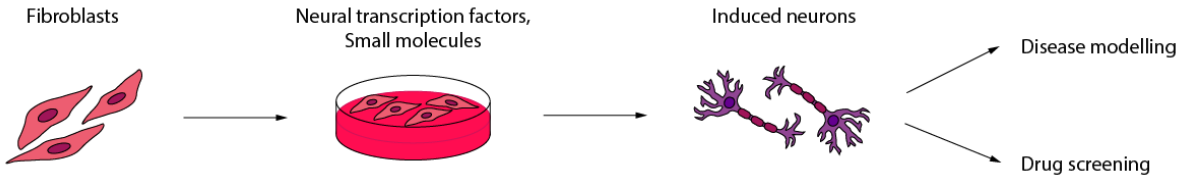

Fig. 1.5 – Representative scheme of neuronal direct conversion.

1.3.4.1. Direct conversion techniques

Most neural direct conversion protocols start with fibroblasts as the donor cell, given the fact that these cells are easily obtained and can stay proliferative *in vitro* for a reasonable number of passages (Pang *et al*, 2011; Pfisterer *et al*, 2011a; Ladewig *et al*, 2012). Many different conversion protocols were successful at generating iNs, raising the number of available protocols for this technique. For example, in 2011, Pfisterer *et al* successfully converted human postnatal fibroblasts using the three BAM factors previously used by Vierbuchen *et al* in the mouse fibroblasts (Pfisterer *et al*, 2011a). On the other hand, Pang *et al* combined this strategy with *NEUROD1* transcription factor and observed an improving in the efficiency of generating human *TUJ-1* positive neuronal cells two to three fold when compared with the BAM factors technique (Pang *et al*, 2011). Besides ectopic expression of transcription factors to mediate lineage conversion, other approaches have been explored such as miRNAs or induction of cellular reprogramming using small molecules (Gopalakrishnan *et al*, 2017). miRNAs have been shown to play an important role in direct reprogramming since they function as repressors of target mRNAs and post-transcriptional regulation of gene expression (An *et al*, 2016). Ambasudhan *et al* showed, in 2011, that the combination of miRNA-124 with *BRN2* and *MYTL1* directly converts postnatal and adult human fibroblasts into functional neurons (Ambasudhan *et al*, 2011). At the same time, Yoo *et al* were able to convert human fibroblasts into neurons using miRNA-9* and miRNA-124 (Yoo *et al*, 2011). Moreover, the addition of the transcription factors *NEUROD2*, *ASCL1* and *MYTL1* improved the conversion efficiency as well as the maturation of the obtained iNs (Yoo *et al*, 2011). Small molecules can also be combined with transcription factor expression and bring advantages to the technique such as enhancement of the reprogramming efficiency and higher

spatial and temporal control of its action, through control of the concentration administered (Li *et al*, 2013). Actually, Ladewig *et al* showed that the efficiency of *ASCL1/NGN2*-induced neuronal conversion was higher upon combination with three molecules that inhibit SMAD, GSK-3β and BMP receptor pathways (Ladewig *et al*, 2012). Liu *et al* were also able to successfully convert human fibroblasts into mature neurons using the transcription factors *NGN2* and *SOX11* along with the small molecules forskolin and dorsomorphin (Liu *et al*, 2013).

1.3.4.2. iNs in neuronal disease modelling

Neuronal cells derived from direct conversion provide a novel platform for diverse applications, including disease modelling (Pfisterer *et al*, 2011a). Characteristics such as speed of conversion, possibility to generate patient-specific cell lines, recapitulation of age-related and disease-related aspects of the patient-derived original cells make direct conversion a very suitable approach for disease modelling. In fact, to the date, several subtypes of neuronal cells have already been converted from human fibroblasts (reviewed in Mertens *et al*, 2016). One neuronal type of clinical importance is motor neurons, which are affected in patients with disorders such as spinal muscular atrophy and amyotrophic lateral sclerosis (Gopalakrishnan *et al*, 2017). In 2011, combining BAM factors with subtype-specific transcriptional cues, Son *et al* generated spinal motor neurons from human fibroblasts, which expressed functional voltage-gated channels and were able to fire action potentials. Another clinically important neuronal subtype is dopaminergic neurons which are affected in patients with Parkinson's disease (Gopalakrishnan *et al*, 2017). Regarding this neuronal subtype it was not only possible to derive human dopaminergic neurons using direct conversion, which may allow to model Parkinson's disease (Pfisterer *et al*, 2011b), but also to derive mouse dopaminergic neurons that were transplanted and able to provide symptomatic relief in a Parkinson's disease mouse model (Kim *et al*, 2011). These studies hold promises for human modelling disease as well as for cell replacement therapy.

At present, neuronal disease modelling is still mostly based on iPSCs system. In any case, it is expected that, within the next few years, the number of disease models using directly converted neurons will increase at a big rate.

1.4. Aims of the study

The aim of the project is to develop a robust human disease modelling system to study Angelman Syndrome. Such a system will serve as a drug testing platform to evaluate, for example, mASO-mediated downregulation of *UBE3A-ATS* to reactivate paternal *UBE3A* gene. For that we have two major objectives:

1. Development of a human model system of Angelman Syndrome, either through neural direct conversion or iPSCs neural differentiation;
2. Characterization of the neuronal identity and imprinted expression of the Angelman locus in the newly-generated cells.

2. Material and Methods

2.1. Cell culture

2.1.1. Punch-skin biopsy fibroblasts

3 year-old Angelman fibroblasts (AS 3y) were obtained from a punch-skin biopsy to a 3 year-old AS patient. After biopsy, skin sample was washed with phosphate-buffered saline 1x (PBS; Sigma Aldrich-Aldrich, Catalog# P3813) with gentle agitation. In a P100 mm petri dish (TPP, Catalog# TPP93100) the subcutaneous tissue was removed by scraping the dermal side using two forceps. The sample was then sectioned into approximately 0.5cm width stripes using a surgical scalpel and it was moved into 6-well plates (TPP, Catalog# TPP92006). 30 year-old Angelman fibroblasts (AS 30y) were previously obtained and expanded the same way by Duarte Brandão (IMM/ MC Fonseca's Lab). Age-matched control fibroblasts (control 30y) were previously derived and provided by Dra. Sofia Duarte (IMM/Centro Hospitalar de Lisboa Central).

Both control 30y and AS 30y fibroblasts were thawed in a 37ºC bath and transferred to a Falcon® tube containing 5mL of fibroblast medium constituted by Dulbecco's Modified Eagle Medium (DMEM; Life Technologies, Catalog# 41966-029) supplemented with 10% Fetal Bovine Serum (FBS; Life Technologies, Catalog# 10270-106), 1mM L-glutamine (Life Technologies, Catalog# 25030-024) and 1% Penincillin/Streptomycin (Pen/Strep; Life Technologies, Catalog# 15070-063). The cells were centrifuged at 1000rpm for 5 minutes and the supernatant was discarded. The pellet was ressuspended in 5mL of fibroblast medium and seeded on a T25 flask (Starsted, Catalog# 833910). When the fibroblasts were approximately 80-90% confluent, the cells were passaged using TrypLE™ Express solution (Life Technologies, Catalog# 12605028). For that, the medium was removed and the cells were washed with 5 mL of PBS and then dislodged through incubation with TrypLE™ Express solution at 37ºC for 3-5 minutes. Cells were then ressuspended with fibroblast medium and seeded in one T75 flask (VWR, Catalog# NUNC156499). Cells continued to be passaged using a 1:2 split ratio to expand the lines. Part of these cells were collected for RNA extraction (see 1.2.4), pelleted or frozen (explained below).

In order to make cell pellets for DNA or RNA extraction, fibroblasts were dislodged using a TrypLE™ Express solution as explained above, transferred to a Falcon® tube and centrifuged at 1000rpm for 5 min. The supernatant was discarded and the pellet was ressuspended in 1mL of PBS and transferred to an Eppendorf tube. After centrifugation at 1000rpm for 5min, the supernatant was discarded. The pellet was snap frozen in liquid nitrogen for a few seconds and stored at -80ºC.

To cryopreserve the cells, after dislodging and centrifugation, the supernatant was discarded and the pellet was ressuspended in freezing medium: 10% dimethyl sulfoxide (DMSO; Sigma Aldrich-Aldrich, Catalog# D2438) in FBS. 1mL of ressuspended cells was transferred to each cryovial (Nunc, Catalog# 366656) and placed at -80ºC. For long storage the cells were placed in liquid nitrogen.

Prior to cryopreservation in liquid nitrogen all cells were tested for the presence of *Mycoplasma*, using MYCOPLASMACHECK service from GATC.

2.1.2. NPCs differentiation from iPSCs

2.1.2.1. iPSCs expansion

iPSC reprogramming of control and AS fibroblasts was performed by Isabel Onofre and Dr. Ana Rita Álvaro in the laboratory of Professor Luís Pereira de Almeida at CNC/UC, using a previously published protocol (Warlich *et al*, 2007). iPSCs expansion and adaptation to feeder-free conditions was performed by Duarte Brandão (IMM/ MC Fonseca's Lab).

For iPSCs expansion in feeder-free conditions, cells were maintained in 6-well plates previously coated with Matrigel (Corning, Catalog# 354230) in mTeSR™1 medium (STEMCELL Technologies, Catalog# 5850) supplemented with 0.5% Pen/Strep. For Matrigel coating, Matrigel was diluted in cold DMEM/F12 (1:30), carefully ressuspended and 1mL of Matrigel-DMEM/F12 was placed in each well of a 6-well plate. The plate was incubated for 2 hours at room temperature or for 30 min at 37ºC before use. Prior to seeding of the cells, Matrigel was removed. Upon high confluency, iPSCs were passaged. For that, cells were washed with 1.5 mL of PBS and incubated 3 minutes with 1mL of 0.5mM EDTA (VWR, Catalog# 0105-1KG) in PBS. After incubation, EDTA was removed, 1.5 mL of mTeSR™1 medium was added to each well and cells were scrapped from the well with a cell scraper. The scrapped cells were collected and transferred to a Falcon® tube containing the volume of mTeSR™1 medium necessary for the desired dilution (usually 1:3). Cells were then seeded in Matrigel-coated wells.

For iPSCs freezing, cells were dislodged using the approach described above and after scrapping cells were transferred to a Falcon® tube containing 1.5 mL of Washing medium [DMEM-F12 (Life Technologies, Catalog# 11039-021) supplemented with 10% of KnockOut Serum Replacement (Life Technologies, Catalog# 10828-028), 1% of non-essential aminoacids (Life Technologies, Catalog# 11140-035), 1mM of L-Glutamine, 0.1mM of β-Mercaptoethanol (Life Technologies, Catalog# 31350-010) and 1% of Pen/Strep]. Cells were centrifuged at 1000 rpm for 3 min, the supernatant was removed and the pellet ressuspended in 250 µL of Freezing medium [10% dimethyl sulfoxide (DMSO; Sigma-Aldrich, Catalog# D2438) in FBS]. This volume was transferred to a cryovial, which was stored at -80ºC. For long storage cells were preserved in liquid nitrogen.

2.1.2.2. Neural Progenitor cells generation and expansion

Neural Progenitor cells (NPCs) were derived from iPSCs following the protocol described in the STEMCELL Technologies Technical Manual – Generation and Culture of Neural Progenitor Cells using the STEMdiffTM Neural System, with adaptations. The Monolayer Culture Protocol was used.

Briefly, iPSCs cultured in mTeSR™1 medium in a P100 mm dish were washed once with PBS and dislodged with EDTA at 37ºC for 10 min. After incubation, 7 mL of DMEM-F12 were added and cells were dislodged by pipetting up and down. For cell counting, 50µL of the cell suspension was mixed with 50µL of Trypan Blue solution (Sigma-Aldrich, Catalog# T-6146) and 10µL were added to a Neubauer chamber. $2x10^6$ cells were seeded in a well of a 6-well plate, previously coated with Matrigel, in 2mL of STEMdiff™ Neural Induction Medium (STEMCELL Technologies, Catalog# 05835) supplemented with 10µM Y-27632 (ROCKi) (STEMCELL Technologies, Catalog# 72302). Medium

was changed daily without ROCKi. Cell passaging was performed upon 80-90% confluency (usually every three days). Dislodging of cells was done through incubation with 1mL of ACCUTASE™ (STEMCELL Technologies, Catalog# 07920) at 37ºC for 10 min. 5mL of DMEM-F12 were added to the cells and they were centrifuged at 300g for 5 min. After discarding the supernatant, pellet was ressuspended in STEMdiff™ Neural Induction Medium with ROCKi. $2x10^5$ cells were seeded into another Matrigel-coated well of a 6-well plate. This process was repeated until passage 2. From passage 3 on, the same protocol was followed, with a split ratio of 1:2.

For NPCs expansion, cells were switched to a Complete STEMdiff™ Neural Progenitor Medium [Basal Medium Catalog# 05834), Supplement A (#05836), Supplement B (#05837)] and passaged upon confluency into a 1:2 split ratio as before. This way NPCs were expanded and part of the generated NPCs was freezed. Usually, cells from a 6-well plate were dislodged and centrifuged. The pellet was ressuspended in 1 mL of NPCs freezing medium (STEMdiff™ Neural Progenitor Medium supplemented with 10% DMSO) and transferred to one cryovial, which was stored at -80ºC and later in liquid nitrogen.

For thawing the cells, one cryovial was thawed into one well of a 6-well plate. For that, the cryovial was thawed in a 37ºC water bath and cells were transferred to a Falcon® tube containing 10 mL of DMEM/F-12 medium. After centrifugation at 300g for 5 min, the pellet was ressuspended in 2mL of Complete STEMdiff™ Neural Progenitor Medium and cells were plated in a previously Matrigel-coated well of a 6-well plate.

2.1.3. Neuronal direct conversion

2.1.3.1. HEK 293T expansion and transfection

HEK 293T cells were thawed and passaged using a 1:2 split ratio following the same procedure as above in HEK medium: DMEM supplemented with 10% FBS, 1mM L-glutamine, 1% Pen/Strep and 1% Non-essencial Aminoacids (NEAA; Thermo Fisher, Catalog# LTID 41966-029). For transfection with lentiviral vectors, cells were dislodged and counted. $2.5x10^6$ HEK 293T cells were seeded per P100 mm dishes previously coated with gelatine (Sigma Aldrich-Aldrich, Catalog# G1890). The day after, transfection was performed: 10µg of each transfer vector - EtO and N2AA - and 5µg of both each packaging vectors - psPAX2 and pMD2G - were mixed and added to 600µL of DMEM and 50µL of X-treme Gene 9 DNA Transfection Reagent (Roche, Catalog# 6365787001). This mixture was vortexed and added to each P100 mm petri dish containing the HEK 293T cells and the transfection took place at 37ºC overnight. After overnight incubation the medium was removed and replaced with fresh medium. 48h later the medium of the transfected HEK 293T cells containing the lentiviruses was collected and filtered using a 0.45µM filters (VWR, Catalog# 514-0075). HEK medium was replaced for a second collection of viral medium for 24 hours.

2.1.3.2. Fibroblasts transduction

Control 30y and AS 30y fibroblasts were plated in wells of 6-well plates and pooled into high densities (80-90% confluency). Fibroblasts transduction was performed by removing the fibroblasts

medium and replacing it with the viral medium collected from the transfected HEK 293T cells. To enhance the infection efficiency, 1µL of polybrene (Santa Cruz Biotechnology, Catalog# SC134220) was added to each 1mL of medium. 24 hours later a second infection was performed with new viral medium. Transduced fibroblasts were expanded in the presence of 200µg/ml G418 (neomycin; Merck. Catalog# 345810) and 1µg/ml puromycin (Sigma-Aldrich, Catalog# P8833) in the first experiment, but given the high efficiency of infection, selection with puromycin and neomycin was not repeated in further experiments.

2.1.3.3. Neural direct conversion

The neural direct conversion was performed according to the protocol by Ladewig *et al* (2012). In summary, the transduced fibroblasts were passaged until high confluency was reached and 24 hours later the medium was changed to Neuron Conversion (NC) medium: DMEM:F12 (Life Technologies, Catalog# LTI11039-021) and Neurobasal medium (Thermo Fisher, Catalog# LTI21103-049) supplemented with N2 supplement (Stem Cell Techonolgies, Catalog# 07152), B27 supplement (Thermo Fisher, Catalog# LTI 17504-044), doxycycline (Sigma Aldrich, Catalog# D9891-1G), laminin (reference), dibutyryl cyclic-AMP (Sigma Aldrich, Catalog# D0627-100MG), human recombinant Noggin (Peprotech, Catalog# 120-10C-100µG), LDN-193189 (Sigma Aldrich, Catalog#SML0559-5MG) A83-1 (Sigma Aldrich, Catalog#SML0788-5MG), CHIR99 021 (Sigma-Aldrich, Catalog# SML 1046-5MG), Forskolin (Sigma Aldrich, Catalog#93049-10MG) and SB-431542 (Sigma Aldrich, Catalog# S4317-5MG). This medium was maintained for three weeks and it was changed every third day. After three weeks, the medium was replaced with Neural Maturation (NM) medium: DMEM:F12/Neurobasal (1:1) supplemented with N2, B27, GDNF (Peprotech, Catalog#450-10-10µG), BDNF (Peprotech, Catalog# 450-02-10µG), dibutyryl cyclic-AMP, doxycycline and laminin for two weeks. Images of the cells undergoing neural conversion were taken at day 3, day 13 and day 27 using a Zeiss Primo Vert microscope.

2.2. Molecular Biology Techniques

2.2.1. Competent cells transformation

Competent cells previously prepared in the lab were transformed with either pLVX-EtO, pLVXTP-N2AA, psPAX2, pMD2.G [kindly provided by J. Mertens (Salk Institute, San Diego, USA)] or GFP plasmids [kindly provided by Edgar Gomes's Lab (IMM, Lisboa, Portugal)]. For that, 2µL of the respective plasmid DNA were added to 100µL of competent cells and the mixture was placed on ice for 30 min. For the heat shock, the mixture was placed at 42ºC for 45 seconds and immediately moved to ice for 2 minutes. 1mL of Luria-Bertani medium (LB) was added and the mixture was incubated at 37ºC for 1 hour, with agitation. After incubation, 100µL of each plasmid mixture was added and scattered in 0,1% ampicillin LB-agar plates (Grisp, Catalog# GAB03.0005), which were left at 37ºC overnight.

Glycerol stock for each plasmid mixture was prepared. For that, one colony from each plate was picked, placed in a 0,1% ampicillin LB-agar plates and incubated overnight at 37ºC, with agitation.

The day after, 150 µL of glycerol (Sigma-Aldrich, Catalog# G6279-500ML) were added to 850 µL of bacteria. The mixture was vortex and stored at -80ºC.

2.2.2. Plasmid DNA extraction

Starting from either 5mL or 400mL culture of bacteria collected from the glycerol stock, plasmid DNA was extracted using the NZY Miniprep Kit (NZYTech, Catalog# MB01002) or the Genopure Plasmid Maxi Kit (Roche, Catalog# 3143422001), respectively, following the manufacturer's protocols. For plasmid restriction digestion to confirm the presence of the correct sequence in the packaging and transfer vectors, DNA was prepared using the NZY Miniprep Kit. On the other hand, for transfection of HEK 293T cells for lentivirus production, plasmid DNA was prepared using the Genopure Plasmid Maxi Kit since this protocol generates much higher yields and better quality of plasmid DNA than NZY Miniprep Kit.

2.2.3. Plasmid restriction digestion

To confirm that the packaging or transfer plasmids glycerol stocks had the correct sequence, each plasmid was digested with restriction enzymes. pLVX-EtO was digested with KpnI (Thermo Fisher, Catalog# FD0524). pLVXTP-N2AA was digested with EcoRI (Thermo Fisher, Catalog# FD0275) and KpnI. psPAX2 was digested with EcoRI and SalI (Thermo Fisher, Catalog# FD0644). pMD2.G was digested with HindIII (Thermo Fisher, Catalog# FD0505) and NotI (Thermo Fisher, Catalog# FD0595). All restriction digestions were performed for 1 hour at 37ºC.

The digestion products were separated on a 0.8% agarose (NZYTech, Catalog# MB05202) gel in 1x Tris-acetate-EDTA (TAE). Digital images were obtained using the Chemidoc XRS+ system (BioRad) and analysed using the Image Lab 5.2 software (BioRad).

2.2.4. RNA isolation from adherent cells and cDNA synthesis

For RNA extraction, cell's medium was removed and 1mL of NZYol reagent (NZYTech, Catalog# MB18501) was added to the cells per $10cm^2$ of culture dish surface and incubated at room temperature for 5 minutes. The mixture was pipetted up and down, transferred to an Eppendorf tube and stored at -80ºC.

For the RNA isolation, 200µL of chloroform were added to the Eppendorf tube. The tube was vigorously shaken for 15 seconds and incubated for 3 min at room temperature, followed by centrifugation at 1200g for 15 min at 4ºC. The aqueous phase was collected into a new tube and 1µL of Glycogen Blue and 500µL of 100% isopropanol were added. The mixture was incubated 10 min at room temperature and centrifuged at 1200g for 10 min at 4ºC. The supernatant was discarded, the pellet was washed with 1mL of 75% EtOH and centrifuged at 7500g for 5 min at 4ºC. The pellet was air-dried for 15 min and ressuspended in 30µL of RNase-free water.

DNase I treatment (Roche, Catalog# 4716728001) was performed on 5µg of RNA according to the manufacturer's protocol with the addition of RiboSafe RNase Inhibitor (Bioline, Catalog# BIO-65027). After, RNA was precipitated by adding 100% EtOH and incubating for 30 min at -80ºC. The

sample was centrifuged at 13000 rpm for 30 min at 4ºC. The pellet was washed with cold 70% EtOH and centrifuged at 13000 rpm for 5 min at 4ºC. After air-dried, the pellet was ressuspended in RNase-free water. RNA concentration was quantified using Nanodrop 2000 (Thermo Scientific).

cDNA synthesis from 500ng of RNA was performed using Transcriptor High Fidelity cDNA synthesis Kit (Roche, Catalog# 5081963001) according to the manufacturer's protocol.

2.2.5. Reverse transcriptase polymerase chain reaction (RT-PCR)

1/15 diluted cDNA product was used as template for RT-PCR in a 25µL reaction volume with BIOTAQ™ DNA polymerase (Bioline, Catalog# BIO-21060) according to the manufacturer's instructions. The primer pairs used are described in Table 2.1. The cycling conditions were: 95ºC for 5 min, then 35 cycles of 95ºC for 30 sec, 60ºC for 30 sec, 72ºC for 20 sec and, finally, 72ºC for 10 min.

RT-PCR products were separated on a 1.5% agarose gel in TAE. The molecular weight marker 1Kb Plus DNA ladder (Invitrogen, Catalog# 10787018) was used. Digital images were obtained and analysed as in section 2.2.3.

Table 2.1 – Primers used for RT-PCR.

Primer	Sequence	Origin
Ascl1 trans F	AGCAGGAGCTTCTCGACTTCACCA	Ladewig *et al*, 2012
Ascl1 trans R	AAGCGCATGCTCCAGACTGCC	Ladewig *et al*, 2012

2.2.6. Reverse-transcriptase quantitative polymerase chain reaction (RT-qPCR)

1/15 diluted cDNA product was used as template for RT-qPCR in a 25 µL reaction volume with - iTaq™ Universal SYBR® Green Supermix (BioRad, Catalog# 1725125) according to the manufacturer's instructions. The primer pairs used are described in Table 2.2. The cycling conditions were: 50ºC for 2 min, 95ºC for 10 min, 95ºC for 15 sec, 60ºC for 1 min, 95ºC for 15 sec, 60ºC for 1 min and 95ºC for 15 sec. RT-qPCR was conducted in Real-Time thermal cycler ViiA7 96-well format or 384-well format (Applied Biosystems). Data was analysed in QuantStudio™ Real-Time PCR Software (Applied Biosystems).

Table 2.2 – Primers used for RT-qPCR.

Primer	Sequence	Origin
Thy1 F	ATCGCTCTCCTGCTAACAGTC	Hu *et al*, 2015
Thy1 R	CTCGTACTGGATGGGTGAACT	Hu *et al*, 2015
Dkk3 F	CTGGGAGCTAGAGCCTGATG	Hu *et al*, 2015
Dkk3 R	TCATACTCATCGGGGACCTC	Hu *et al*, 2015
Sox2 F	ATGCACCGCTACGACGTGA	Liu et al, 2012
Sox2 R	CTTTTGCACCCCTCCCATTT	Liu et al, 2012
Oct4 F	CTGAGGGCGAAGCAGGAGTC	Jezierski *et al*, 2010
Oct4 R	CTTGGCAAATTGCTCGAGTT	Jezierski *et al*, 2010
Nanog F	GCAGAAGGCCTCAGCACCTA	Jezierski *et al*, 2010
Nanog R	AGGTTCCCAGTCGGGTTCA	Jezierski *et al*, 2010
Nestin F	CAGCGTTGGAACAGAGGTTGG	Haase *et al*, 2009

Nestin R	TGGCACAGGTGTCTCAAGGGTAG	Haase *et al*, 2009
Map2 F	CCACCTGAGATTAAGGATCA	Dueñas *et al*, 2014
Map2 R	GGCTTACTTTGCTTCTCTGA	Dueñas *et al*, 2014
Tuj1 F	GCCTCTTCTCACAAGTACGTGCCTCG	MC Fonseca Lab homemade
Tuj1 R	GGGGCGAAGCCGGGCATGAACAAGAAGTGCAG	MC Fonseca Lab homemade
GFAP F	GTACCAGGACCTGCTCAAT	MC Fonseca Lab homemade
GFAP R	CAACTATCCTGCTTCTGCTC	MC Fonseca Lab homemade
Gapdh F	GTCGTGGAGTCCACTGGCGTC	Hogart *et al*, 2007
Gapdh R	TCATGAGTCCTTCCACGATAC	Hogart *et al*, 2007

2.3. Cellular characterization

2.3.1. RNA Fluorescent *in situ* hybridization (RNA-FISH)

SNORD116 probe was made from BAC RP11-186C7 (BACPAC Resources Center) and prepared using Nick Translation Kit (Abbot, Catalog# 07J00-001) with Green dUTP (Enzo Life Sciences, Catalog# 53202N32-050). Custom Stellaris™ RNA FISH probes for *UBE3A* were designed using the Stellaris™ Probe Designer software (Biosearch Technologies) and prepared with Quasar® 570 Dye (Biosearch Technologies, Catalog# SMF-2038-1).

SNORD116 BAC probe was precipitated with 1 mg/ml human sonicated DNA, 1 µg/µl human Cot1 DNA (Thermo-Fisher, Catalog# 15279011), 3M Sodium Acetate (NaAc; Sigma-Aldrich, Catalog# S2889-1KG) and EtOH 100%. The mixture was vortex and centrifuged for 30 min at 12500 rpm at 4ºC. The supernatant was removed and the pellet washed with 1ml of cold EtOH 70% and centrifuged for 5 min at 12500 rpm at 4ºC. The pellet was air dried for 15 min and diluted in Formamide (FA; Fisher Scientific, Catalog# 10602882). The probes were placed at 37ºC for 15 min, 75ºC for 15 min and 37ºC for 30 min with agitation and placed on ice.

In parallel, fibroblasts, iPSCs or NPCs previously cultured on 6-well plates with gelatine-coated coverslips or matrigel-coated coverslips (22x22mm; Normax, Catalog# 5470004A) for 24 hours, were washed with 2mL of PBS 1x and fixed using Fixative solution [3.7% paraformaldehyde (PFA; Merck Millipore, Catalog# 1040051000)] for 10 min at room temperature. After this, cells were washed with 1x PBS and permeabilized on ice for 5 min using Permeabilization Buffer [1x PBS, 0.5% Triton x100 (Sigma-Aldrich, Catalog# T8787-50ML) and 1% vanadyl ribonucleoside complex (VRC; Sigma-Aldrich, Catalog# 94742-10ML)]. Next, cells were washed with 70% ethanol and incubated 1 hour with 70% ethanol at room temperature. After incubation, cells were washed with Wash Buffer [20x saline-sodium citrate (SSC, 17,53% (p/v) NaCl and 8,82% (p/v) dihydrate trisodium citrate in RNase-Dnase free water), FA and DNase-RNase free water] for 10 min at room temperature. Humid chamber was prepared with Wash Buffer. Each coverslip was transferred to one slide with 25µL of Hybridization Buffer [50% Dextran Sulfate (Milipore, Catalog# S4030), 20x SSC and FA] (containing 0,25 µL of *UBE3A* probe and 2,5 µL of *SNORD116* probe per coverslip) and incubated overnight on the humid chamber at 37ºC. The day after, coverslips were washed 2 times at 37ºC for 30 min in Wash Buffer and one time at room temperature for 5 min with 2xSSC. DNA counterstaining was performed for 5 min at room temperature in 2xSSC containing 0.2mg/ml of 4',6-diamidino-2-phenylindole (DAPI; Sigma Aldrich-Aldrich, Catalog# D9542) and the coverslips were washed 2 times for 5 min at room

temperature with 2xSSC. Finally, coverslips were mounted in 4µL of mounting medium [PBS 10X, p-phenylenediamine (Sigma-Aldrich, Catalog# 695106), glycerol] and sealed with nail polish. Cells were observed with the wide-field fluorescence microscope Zeiss Axio Observer (Carl Zeiss MicroImaging) with 63x oil objective using the filter sets FS43HE, FS38HE and FS49. Digital images were analysed with the FIJI software.

2.3.2. Immunofluorescence (IF)

For IF, cells were previously cultured on 6-well plates with gelatine-coated coverslips or matrigel-coated coverslips for 24 hours. Cells were washed once with PBS 1x and fixed with PFA 3.7% for 10 min at room temperature. After incubation, cells were washed 2 times with PBS 1x and permeabilized with Permeabilization buffer (Triton 0.1% and PBS 1x) for 5 min on ice. After one wash with PBS 1x, cells were treated with Blocking Solution (BSA 1% in PBS 1x) for 20 min at room temperature. The primary antibody – TUJ1 (BioLegend, Catalog# 801201), NANOG (eBioscience, Catalog# 14-5768-80), SOX2 (Citomed, Catalog# MAB2018-SP), OCT4 (Merck Millipore, Catalog# MAB4419) or NESTIN (R&D systems, Catalog# IC1259P) - was diluted in the Blocking Solution and 15µL of it were added to parafilm inside a humid chamber. Coverslips were transferred to the parafilm and incubated 1 hour to overnight at 4ºC. Cells were washed three times with PBS 1x for 5 min each wash and then incubated with de secondary antibody - Cy™3 AffiniPure F(ab')$_2$ Fragment Goat Anti-Mouse IgG (H+L) (Jackson ImmunoResearch Laboratories Inc., Catalog# 115-166-003) - for 1 hour in the humid chamber, at 4ºC. After incubation, cells were washed 3 times with PBS 1x for 5 min each wash and DNA counterstaining was performed with 0.2mg/ml of DAPI for 2 min. Finally, coverslips were transferred to the slide containing 15µL of Vectashield mounting medium (Vectorlabs, Catalog# H-1000). Imaging was performed as for section 2.3.1.

3. Results and Discussion

In order to establish an *in vitro* human model system for Angelman syndrome, it is necessary to, first, be able to generate neuronal cells derived from AS patients. For that, we considered two possible routes: direct neural conversion and neural differentiation from iPSCs. Given the interest of time, we initially favoured the neural direct conversion protocol. Indeed, neural direct conversion takes about three weeks to obtain induced neurons, plus one week for further maturation, while iPSCs differentiation takes about four to six months to obtain differentiated neurons. Therefore, we decided to try to establish for the first time a neuronal direct conversion protocol in our laboratory in order to generate neuronal cells with the purpose of developing a reliable human model for AS. Once generated, and in order to constitute a reliable AS model system, AS patient-derived and control neuronal cells have to present the correct imprinted expression of the Angelman locus, *i. e*., no expression of *UBE3A* in AS patient-derived neurons and expression of *UBE3A* from only one allele in control neurons.

3.1. Neural Direct Conversion

Within direct neural conversion, several protocols using different transcription factors and small molecules had already been successfully attempted. We decided to follow Ladewig *et al* (2012) protocol, using *ASCL1* and *NGN2* neural transcription factors and a small molecule cocktail medium, since it presented, at the time, the higher conversion efficiency. Briefly, in this protocol, fibroblasts are infected with doxycycline-inducible lentiviruses that drive the expression of the two neural specific transcription factors: *ASCL1* and *NGN2*. For conversion, the infected fibroblasts are maintained for three weeks in a conversion medium composed by small molecules that include SMAD pathway inhibitors (e.g. recombinant human Noggin, LDN-192189, A83-1 and SB-431542), to obtain induced neurons. These iNs are then maintained for one week in a maturation medium containing neurotrophic factors (e.g. BDNF and GDNF) in order to obtain mature neurons.

The first step in neural direct conversion protocol was the production of 2nd generation lentiviruses (Fig. 3.1 A). In its simpler form, this is a three-plasmid system composed by a transfer vector with the desired insert, a packaging vector containing *Gag*, *Pol*, *Pro*, *Rev* and *Tat* genes from HIV genome – the psPAX2 plasmid - and an envelope vector encoding for VSV-G envelope protein – the pMD2.G plasmid - (Merten *et al*, 2016) (Fig. 3.1 B). Neural direct conversion specifically requires two transfer vectors: one vector with the Tet-On Advance system – the pLVX-EtO plasmid -, that is, a reverse tetracycline-controlled transactivator (rtTA), and one vector with the Tet Response element (TRE) driving expression of two neural-specific transcription factors: *ASCL1* and *NGN2* – the pLXTTP-N2AA plasmid (Fig. 3.1 B). In the presence of tetracycline, or it's derivate, doxycycline (dox), rtTA binds to TRE and activates transcription of *ASCL1* and *NGN2* transcription factors.

First, we transformed competent E. coli (DH5α) cells for each plasmid and two independent clones were submitted to plasmid DNA extraction and restriction digestion (Fig. 3.1 C). All the duplicates presented the expected digestion products except pLVX-EtO clone 2 whose digestion was not successful (Fig. 3.1 C).

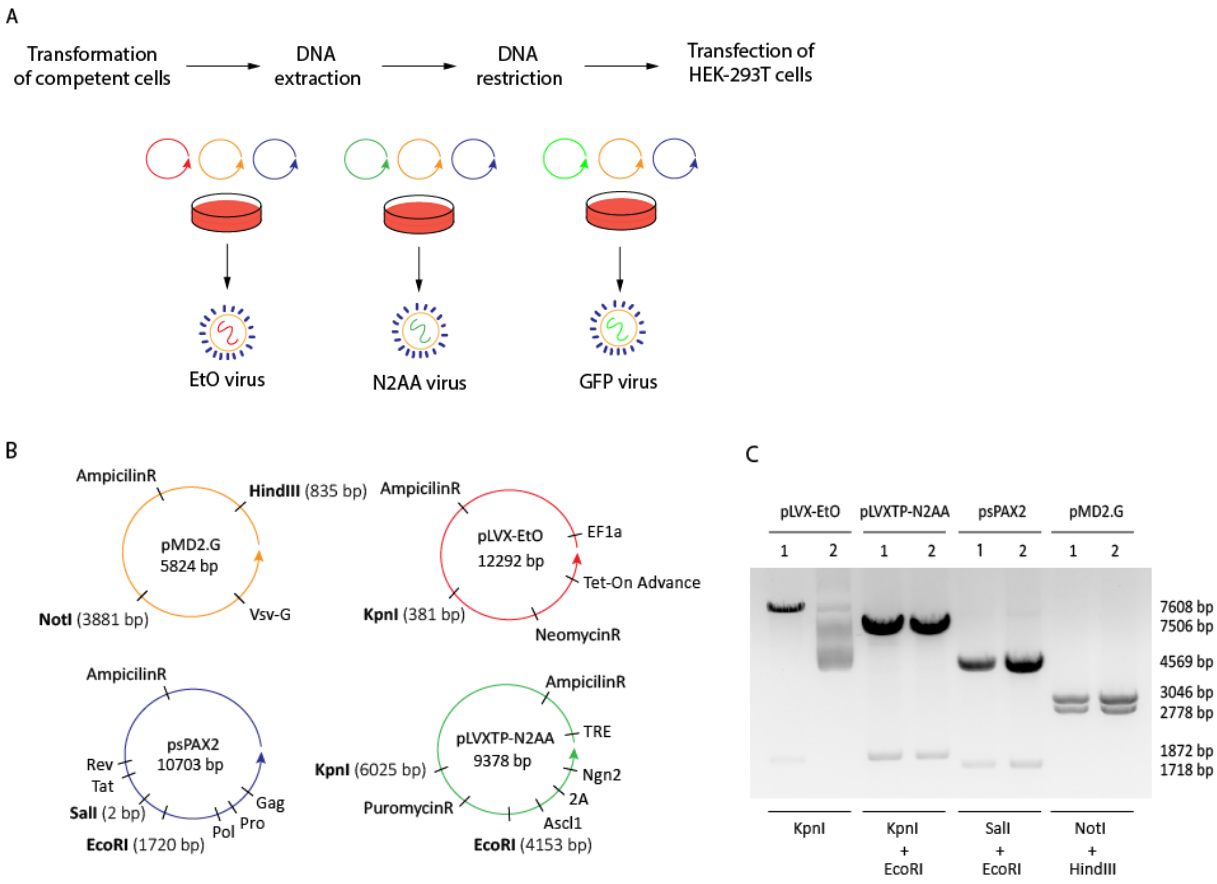

Fig. 3.1 - Characterization of the plasmid vectors used for neural conversion. A – Workflow from transformation of the plasmid vectors into competent bacteria to production of the EtO and N2AA lentiviruses. B – Schematic representation of the pMD2.G, psPAX2, pLVX-EtO and PLVXTP-N2AA plasmids. C – Restriction digestion of pMD2.G, pLVX-EtO, psPAX2 and PLVXTP-N2AA plasmid DNA.

In order to produce the lentiviruses, HEK 293T cells were transfected with the packaging vector (psPAX2), the envelope vector (pMD2.G) and a transfer vector, either the pLVX-EtO plasmid or the pLVXTP-N2AA plasmid to generate EtO and N2AA lentiviruses, respectively (Fig. 3.1 A). We also transfected these cells with a transfer vector containing a Green Fluorescent Protein (GFP) plasmid to obtain lentiviruses expressing a GFP protein to be used as a control for the efficiency of lentiviral infection. The EtO, N2AA and GFP lentiviruses were initially used to infect fibroblasts derived from a 3 years-old AS patient (Fig. 3.2 A). Infection efficiency was high since most nuclei were stained for GFP (Fig. 3.2 B). Even though, no quantification assay was conducted, we estimated that more than 80% of the cells were GFP-positive. EtO and N2AA lentiviruses were initially used for infection separately in order to control for the plasmids response to antibiotic selection, or together as part of the neuronal direct conversion protocol. Two days after infection, selection was initiated. Fibroblasts infected with only EtO or N2AA lentiviruses were selected with puromycin or neomycin, respectively, while fibroblasts infected with both lentiviruses were selected with both puromycin and neomycin. Non-infected fibroblasts were used as negative controls for puromycin and/or neomycin selection. As expected, selection with puromycin and/or neomycin did not affect the infected fibroblasts, as they were maintained confluent until day 7 under selection, with negligible cell death (Fig. 3.2 B) and survived cell passaging at day 7 with a 1:2 split ratio. In contrast, non-infected fibroblasts died under

selection with puromycin and/or neomycin (Fig. 3.2 C). Interestingly, we could also observe that selection with puromycin was far more efficient than with neomycin. Massive cell death was already observed at day 6 and no cells survived until day 11 under puromycin selection. In contrast, neomycin caused cell death was barely observed until day 6, but by day 11, no viable cells were left.

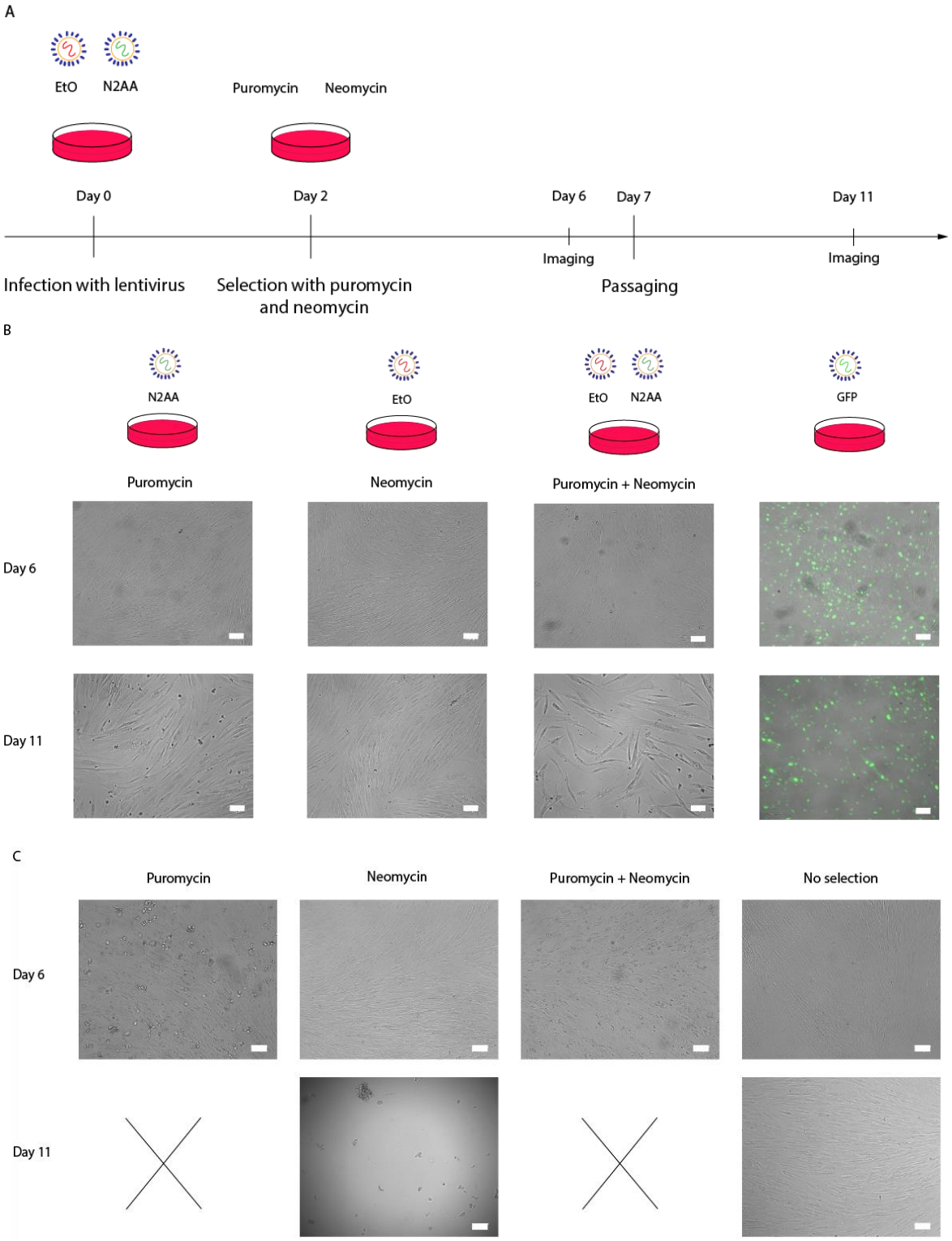

Fig. 3.2 - Infection and selection of AS 3y fibroblasts with lentivirus for neural conversion. A – Experimental timeline for the infection, selection and imaging of the infected and non-infected fibroblasts. B – Representative images of infected AS 3y fibroblasts with N2AA, EtO and both N2AA and EtO under selection and GFP-infected fibroblasts without selection at day 6 and

day 11. Scale bar: 100μM. C – Representative images of non-infected fibroblasts under selection with puromycin, neomycin, a combination of both and under no selection. Scale bar: 100μM.

Even though infected fibroblasts with both EtO and N2AA survived, we noticed that they became slower at dividing and cells started to show a flatten morphology reminiscent of cells undergoing cell senescence (data not shown). Given the high efficiency of infection, reflected from the great number of cells exhibiting GFP expression, we decided to skip the selection step in further experiments.

The previous experiments were conducted to test both the infection of fibroblasts with newly-produced lentiviruses and the antibiotic selection in AS 3y fibroblasts. For the actual neural direct conversion, we used control and AS fibroblasts from 30 years-old female individuals. Given that this biological material was precious and not ilimited we decided not to run these tests in those cells.

In a second round of experiments, both control and AS 30y fibroblasts were infected with EtO and N2AA lentiviruses and subjected to neural direct conversion according to the protocol described by Ladewig *et al* (2012). Five days after infection, control and AS 30y fibroblasts medium was replaced with NC medium with dox (day 0) for 21 days in order to generate immature iNs (Fig. 3.3 A). NC medium is composed by 11 compounds: recombinant human Noggin, LDN-192189, A83-1, SB-431542, CHiR99021, forskolin, dibutyryl cyclic-AMP, N2 supplement, B27 supplement, doxycycline and laminin. Briefly, recombinant human Noggin, LDN-192189, A83-1 and SB-431542 are antagonists of bone morphogenetic proteins, while CHiR99021 is a GSK-3β inhibitor. Forskolin and dibutyryl cyclic-AMP are a cAMP production enhancer and a cAMP analog, respectively. N2 supplement allows neural commitment and differentiation, while B27 supplement helps survival, growth and maturation of neurons in culture. Laminin, which is commonly used to coat tissue culture dishes for culture of neuronal cells, was supplemented in NC medium since laminin coating tends to get consumed by the cells upon large culture time. Finally, doxycycline is used for induction of the cassette containing *ASCL1* and *NGN2* transcription factors. During this phase of conversion the recombinant human Noggin concentration in NC medium was inadvertently incorrect, being 4 times lower than described in the protocol. At day 21, NC medium was replaced with NM medium in order to obtain mature iNs. In neural maturation medium, the BMP and GSK-3β pathway inhibitors are replaced with BDNF and GDNF, which are neurotrophic factors that regulate neural survival and promote neural maturation. The neural direct conversion process was followed by imaging of the cells (Fig. 3.3 B). At day 3, a remarkable morphological change was observed in both control and AS 30y cells (Fig. 3.3 B and 3.3 C). This morphological change was reminiscent of changes noticed previously using the same protocol (Ladewig *et al*, 2012). Morphology changes continued to occur, although less abruptly, from day 13 to day 27 (Fig. 3.3 B). Importantly, from day 13 onwards differences between control and AS 30y cells morphology were easily perceived. This could be due to the progressive dislodging that AS 30y cells suffered along the process, which may impact on neural conversion. This low attachment of the converting AS 30y cells also posed as an obstacle to the downstream imaging experiments.

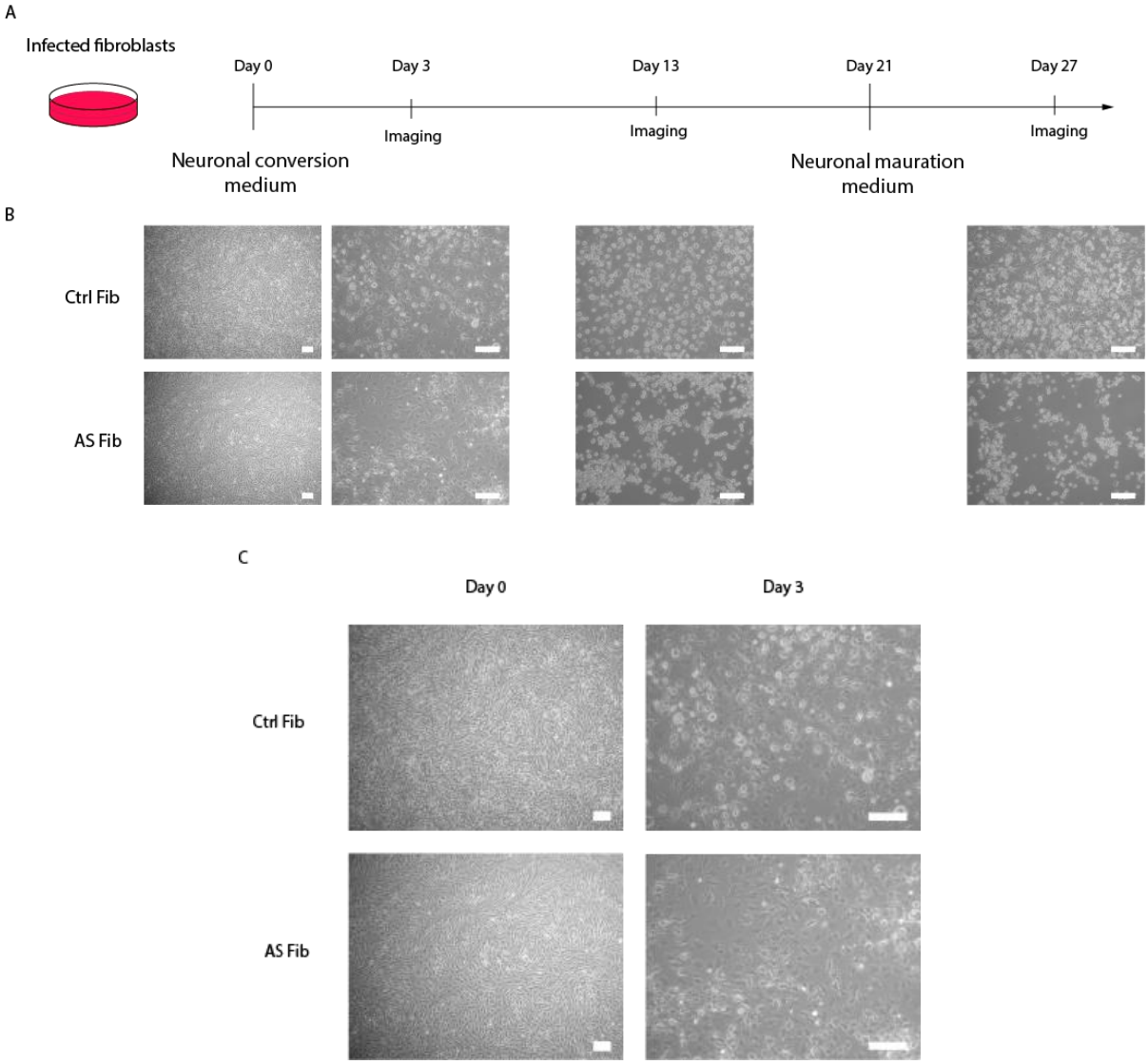

Fig. 3.3 - Neural direct conversion of control and AS 30y fibroblasts. A – Timeline of neural direct conversion protocol indicated the time-points for imaging. B – Representative images of infected control and AS fibroblasts under neural direct conversion Scale bar: 50µM. C – Magnification of the representative images in Fig. 8B for day 0 and day 3.

In order to confirm the expression of inserted *ASCL1* transcription factor in the converted cells, RT-PCR was conducted in control and AS 30y iNs at day 28 of differentiation, as well as in control and AS 30y fibroblasts. Due to the inexistence of primers that distinguish the endogenous from the transgenic *NGN2*, the same analysis was not performed for *NGN2* transcription factor. *GAPDH* was used as a housekeeping control gene. Expression of transgenic *ASCL1* was observed in control and AS 30y iNs but not on the original fibroblasts, as expected (Fig. 3.4). These results confirmed the insertion and the dox-inducible expression of the *ASCL1* lentiviral cassette.

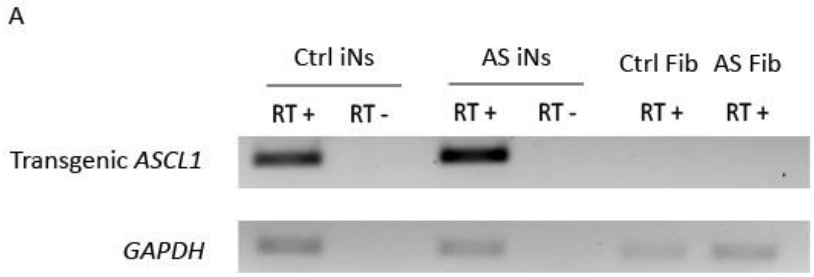

Fig. 3.4 -RT-PCR for transgenic *ASCL1* in control 30y iNs (Ctrl iNs), AS 30y iNs (AS iNs), control 30y fibroblasts (Ctrl Fib) and AS 30y fibroblasts (AS Fib). *GAPDH* was used as housekeeping control gene (RT+ and RT– represent cDNA synthesis in the presence or absence of the reverse transcriptase enzyme, respectively).

Next, in order to characterize the converted cells and unravel their identity we analysed the expression of the fibroblast-specific genes *DKK3* and *THY1* and the neuronal-specific gene *MAP2* by RT-qPCR.

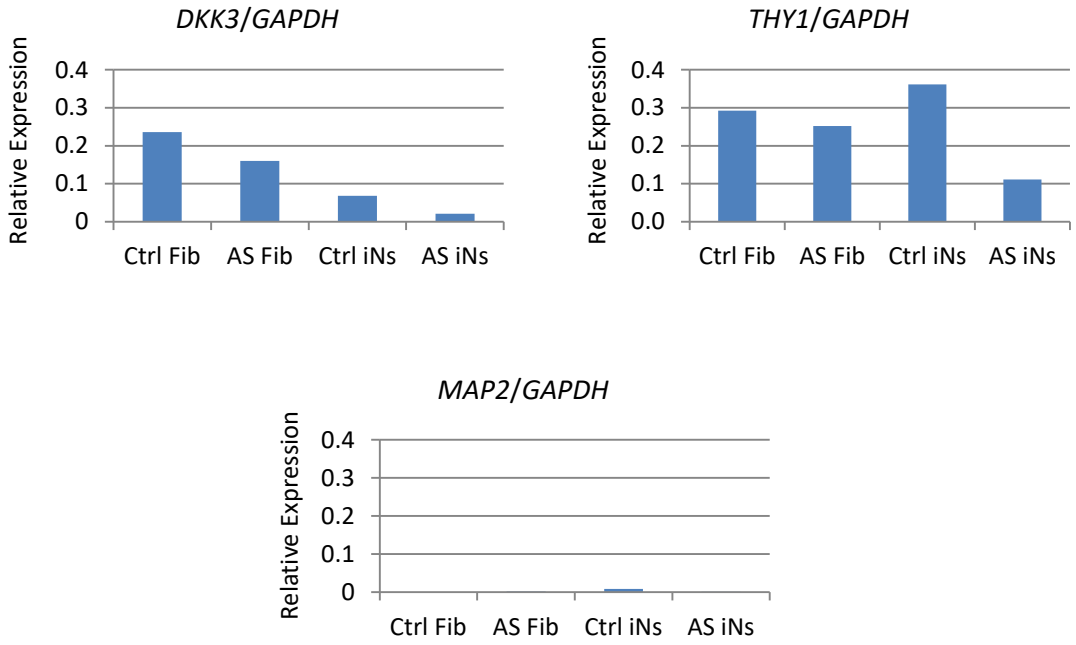

Fig. 3.5 - RT-qPCR analysis of the relative expression of the fibroblast-specific genes *DKK3* and *THY1* and the late neuronal-specific gene *MAP2* in control 30y fibroblasts (Ctrl Fib), AS 30y fibroblasts (AS Fib), control 30y iNs (Ctrl iNs) and AS 30y iNs (AS iNs). *GAPDH* was used as a housekeeping control gene.

Although *DKK3* expression was, as expected, lower in control and AS iNs than in the original fibroblasts, the same was not observed for *THY1* expression, whose expression in control iNs was slightly higher (Fig. 3.5). This suggests that control iNs did not completely lost the fibroblast phenotype, at least, in a proportion of cells. In the case of AS iNs, both *DKK3* and *THY1* genes seemed to be downregulated, as expected. We also monitored the expression of the neural-specific *MAP2* gene, which is normally associated with advanced stages of differentiation. *MAP2* gene was

found to be more expressed in control iNs when compared to the original fibroblasts, which is suggestive of some degree of neuronal conversion. In contrast, AS iNs did not show any *MAP2* induction. Despite reduced fibroblasts-specific gene expression, AS iNs do not show signs of neuronal-like identity. This might be associated to the progressive dislodging that AS 30y suffered during neuronal conversion protocol (Fig. 3.3 B and C). In summary, the RT-qPCR results were unclear concerning the differentiation state of the converted cells.

Since Noggin concentration was inadvertently lower in the first neural conversion experiment, we decided to do a second experiment using the rectified Noggin concentration in the NC medium. In this second round, percentage of GFP-positive cells upon infection of fibroblasts with lentivirus containing the GFP cassette was quantified by FACS-sorting. Approximately 60% of the cells were GFP-positive. However, this measurement was conducted 22 days after GFP infection and may not translate the real percentage of GFP-stained fibroblasts upon infection, which might have been higher. In parallel, we decided to use an additional control, consisting on culturing non-infected fibroblasts in NC medium to control for putative cell morphology changes caused solely by this medium. Surprisingly, AS 30y non-infected fibroblasts also underwent morphological changes similar to the ones observed for fibroblasts infected with N2AA and EtO lentiviruses (Fig. 3.6 A). These result prompted to the hypothesis that the NC medium alone may be responsible for the drastic morphology changes observed in the converting cells and that those changes were not necessarily result from expression of *ASCL1* and *NGN2* transcription factors. In any case, we pursued with the neural direct conversion protocol with the correct dosage of Noggin. Again, dislodging of the AS 30y converting cells continued to be observed, and, moreover, it was also observed for control 30y cells. This suggests that low attachment capability may be a characteristic of cells under neuronal conversion in our conditions, and, therefore, a drawback of this approach.

At day 40 of differentiation, we analysed the expression of the fibroblasts-specific gene *THY1* and the neuronal-specific genes *TUJ1* and *MAP2* by RT-qPCR. In this analysis we included samples of iPSCs-derived neurons with 35 days [kindly provided by Teresa Silva (IMM/ MC Fonseca's Lab)] and with 123 days [kindly provided by Dra. Cláudia Gaspar (IMM/ Domingos Henrique's Lab)] as positive controls for the neuronal-specific genes. *THY1* was expressed, as expected, by both control and AS fibroblasts and almost not expressed by both iPSC-derived neurons. However, in iNs, *THY1* expression was detected, being expressed even slightly higher in control iNs (Fig. 3.6 B). The results suggest that iN derived in this second experiment did not completely lost their fibroblast identity. *TUJ1* expression, an early neural-specific marker gene usually detectable at day 23 of differentiation with this protocol, was higher in iPSCs-derived neurons with 35 days, which are relatively immature (Silva *et al*, unpublished), being lower in iPSCs-derived neurons with 123 days, as expected. Both control and AS 30y fibroblasts also presented some *TUJ1* expression (Fig. 3.6 B), but lower than 35 days iPSCs-derived neurons. However, its expression in iNs was markedly low, not even being detected in AS iNs (Fig. 3.6 B) which is, again, suggestive that iNs did not showed signs of neural fate, not even with an immature phenotype. Finally, we analysed *MAP2* expression. *MAP2* was expressed by 35 days iPSCs-derived neurons and was further increased upon 123 days of neuronal differentiation of iPSCs (Fig. 3.6 B) as expected since *MAP2* is a late neuronal-specific gene. *MAP2* was very lowly

expressed in control 30y fibroblasts (not detected in AS 30y fibroblasts) and, again, both control and AS iN only showed very modest levels of *MAP2* (Fig. 3.6 B). Overall, the RT-qPCR results do not indicate that the fibroblasts acquired neuronal identity. However, these results were obtained using a population-averaged approach such as RT-qPCR, and, therefore, we could not discard that a few cells could have indeed acquired a neuronal fate.

To investigate that we decided to perform an IF assay on control and AS 30y iNs for *TUJ1*, vastly used as an early neural-specific gene. Surprisingly, under our IF conditions, we could detect *TUJ1* signal in both AS 30y fibroblasts and AS 30y iNs (Fig. 3.6 C). Data for control 30y cells is not shown due to the major dislodging of the iNs from the coverslips, which happened in both iNs cell lines, being Fig. 3.6 C one of the few examples obtained. The detection of *TUJ1* in AS 30y fibroblasts prevented us from confirming the neural or non-neural identity of the converted cells by IF. *TUJ1* is normally used to detect neuronal differentiation from iPSCs however, herein, we used it to assess the neural identity of cells directly converted from fibroblasts. Therefore, we controlled *TUJ1* staining by performing IF in AS 30y fibroblasts, expecting no staining. The detection of *TUJ1* in AS 30y fibroblasts by IF is, in fact, in agreement with the RT-qPCR results for *TUJ1* expression in both control and AS 30y fibroblasts. It would be interesting to perform the same IF in neuronal cells to understand if the result would be a similar or a much higher staining of *TUJ1*.

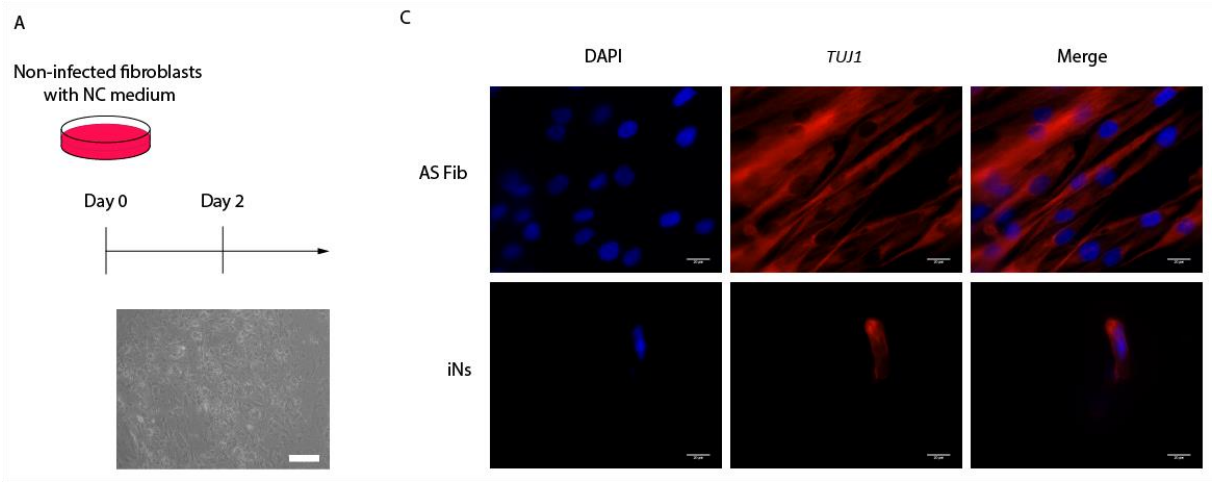

B

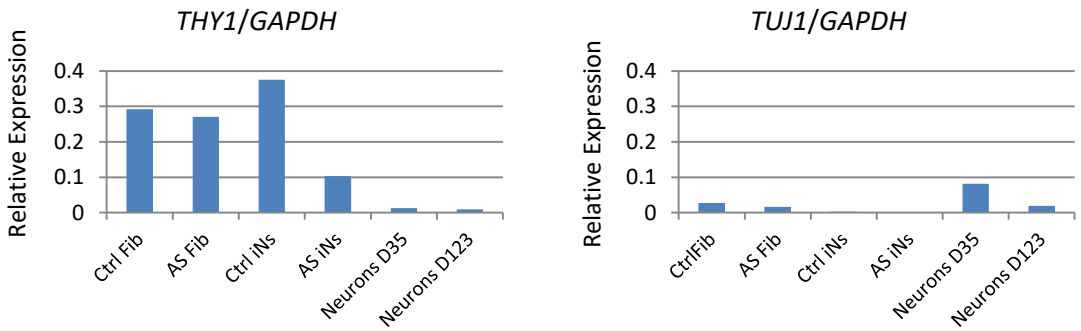

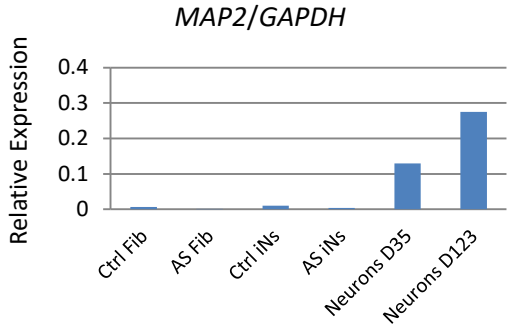

Fig. 3.6 - 2nd round of neural direct conversion of control and AS 30y fibroblasts. A – Representative image of non-infected fibroblasts maintained in NC medium at day 2. Scale bar: 50 µM. B – RT-qPCR analysis of the relative expression of the fibroblast-specific gene *THY1*, the early neuronal-specific gene *TUJ1* and the late neuronal-specific gene *MAP*2 in control 30y fibroblasts (Ctrl Fib), AS 30y fibroblasts (AS Fib), control 30y iNs (Ctrl iNs), AS 30y iNs (AS iNs), iPSCs-derived neurons with 35 days (Neurons D35) and iPSCs-derived neurons with 123 days (Neurons D123). *GAPDH* was used as a housekeeping control gene. C – Representative images of IF assay for *TUJ1* in AS 30y fibroblasts and AS 30y iNs. Scale bar: 20µM.

Overall, characterization of both control and AS 30y iNs suggested that the infected fibroblasts subjected to neural direct conversion, or at least the great majority of them, did not acquired neuronal identity. Although we were following an optimized neural direct conversion protocol, several aspects may explain the failure in obtaining iNs. Despite following the protocol of Ladewig *et al* (2012), due to laboratory condition constrains, two alterations were made to it. First, in the original 2nd generation lentiviral protocol followed by Ladewig and colleagues, the authors performed concentration of the lentiviruses by either ultracentrifugation or low speed centrifugation overnight. Besides concentrating the virus and enhancing the infection efficiency, centrifugation allows purification of the viral medium with which fibroblasts are infected (Koch *et al*, 2006). In fact, the viral medium used to infect the fibroblasts was previously used to culture HEK 293T for 24 hours in order to produce the viruses and, therefore, some of the components are partially consumed and the medium contains cell products of metabolism. This was an optional step in the protocol that we decided not to perform since infection efficiency controlled through GFP infection was high. Despite optional, this step could have increased the infection efficiency [by ~3-fold, according to Koch *et al* (2006)] which could have a big impact in the number of cells that acquire neural identity. The second alteration to the protocol consisted in skipping the double puromycin/neomycin selection. As already explained above, upon selection we noticed a senescence-like morphology and a reduction in cell division rate which led us to decide to skip the selection step. It could be that skipping the antibiotic selection step resulted in smaller number of cells expressing the Dox-inducible cassette with *ASCL1-NGN2*. Given the high percentage of GFP infection, this seems not be the case. Furthermore, we also detected expression of transgenic *ASCL1* in the infected fibroblasts. In any case, it might be that the selection step would select for cells expressing higher levels of transgenic cassette, which in the absence of selection resulted in cells expressing lower levels of the *ASCL1-NGN2* transcription factors, which were insufficient for cell conversion into neurons.

Another important aspect which was sub-optimal in this experiment was the frequent dislodging of cells from PLO/laminin–coated dishes which posed as a problem for both maintenance of cells in

culture and imaging. This problem was approached by trying different coatings, usually recommended for neuronal cells culture, such as Poly-L-Lysine and matrigel. Although cellular detachment persisted, it was slightly decreased with matrigel coating, therefore, imaging of iNs was performed with matrigel-coated coverslips. Nevertheless, we could notice that upon matrigel coating, iNs would present a wrinkled morphology, as it was possible to observe in IF assay for *TUJ1* (Fig. 3.6 C).

Finally, it should not be discarded the hypothesis of a possible mixed-population, with a minority of cells having neural identity. To asses this question, FACS-sorting for neuronal cells could be performed on the generated iNs, which could be further characterized. In any case, if neuronal conversion had occurred in a minority of cells, the scarcity of converted cells precludes the use of this method as a suitable model system to study Angelman Syndrome.

3.2. iPSCs differentiation

Due to the unsuccessful generation of proper induced neurons with our adapted direct conversion protocol, we decided to try to generate neurons through iPSCs differentiation. Reprogrammed iPSCs differentiation also allows the generation of neurons, through recapitulation of developmental stages, with the first step being their induction into neural progenitor cells. (Fig. 3.7 A). When compared with direct conversion, iPSC differentiation presents higher conversion efficiency (Kwon *et al*, 2016) and it is also a vastly studied field with higher number of available and successful protocols. Also, it gives a developmental component suitable to study neurodevelopmental diseases such as AS (Nikoletopoulou and Tavernarakis, 2012). However, as explained above, it is a very time-consuming approach, since it takes almost one month to obtain neural progenitor cells plus differentiation and maturation time. This was the reason for having iPSCs differentiation as second choice to generate patient-derived neurons.

Starting with the established control iPSC line by Duarte Brandão (iMM) we decided to induce them into NPCs (Fig. 3.7 B), using the STEMCELL Technologies monolayer protocol (Fig. 3.7 C). This protocol was chosen giving the fact that is a very simple and optimized commercially available protocol. Within this protocol, neural progenitor cells can be generated through a monolayer protocol or an embryoid bodies protocol. The monolayer protocol was chosen since it is a simpler protocol with less troubleshooting and also due to the lack of material for embryoid bodies generation in our laboratory, such as, AgreeWell™ 800, which are recommended for successfully generating iPSC-derived EBs for neural induction. Following the STEMCELL Technologies monolayer protocol, iPSC single cells were plated in STEMdiff™ Neural Induction Medium in the presence of ROCKi for 24h and then maintained in the same medium without ROCKi for 19 days. During this time, cells were passaged in a 1:2 split ratio. Nineteen days later, cells were switched for STEMdiff™ Neural Induction Medium in order to expand the generated NPCs. Passages were also performed in a 1:2 split ratio for 23 days. Cells were then collected for characterization through RT-qPCR and IF. The generation of NPCs was conducted with the help of Duarte Brandão.

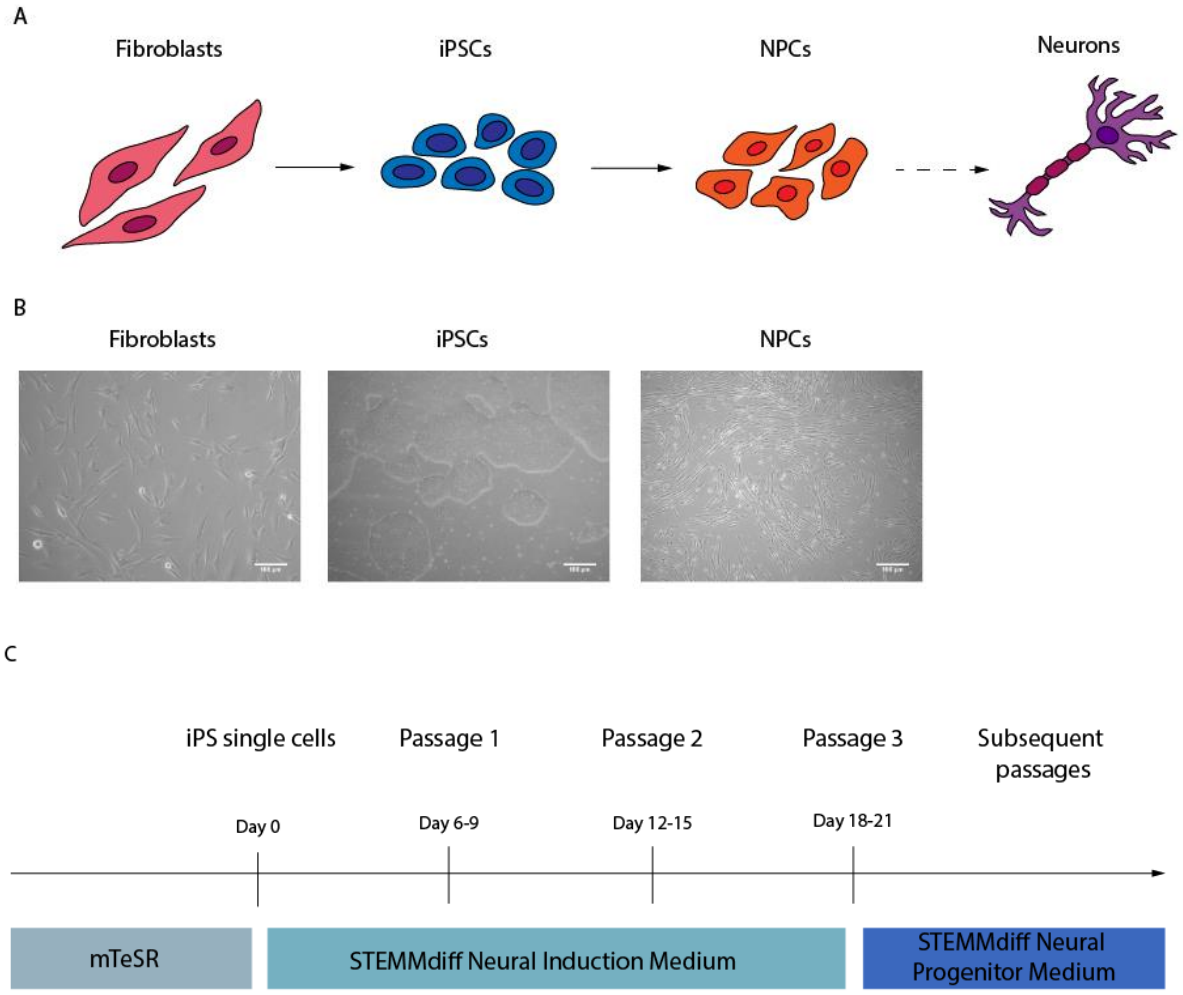

Fig. 3.7 - iPSCs reprogramming and neural differentiation. A – Representative scheme of reprograming of fibroblasts into iPSCs and their differentiation into NPCs and, finally, functional neurons. B – Representative images of fibroblasts reprogrammed iPSCs and NPCs. Scale bar: 10μM. C – Representative scheme of NPC generation and expansion from iPSCs according to STEMCELL Technologies monolayer protocol.

To assess the pluripotency of the generated control iPSCs, IF experiments were conducted using antibodies against the stem cell markers *NANOG*, *SOX2* and *OCT4*. The generated control NPCs were also characterized by an IF assay using antibodies against *NANOG* (iPSCs^{+}, NPCs^{-}), *SOX2* (IPSCs^{+}, NPCs^{+}) and *NESTIN* (IPSCs^{-}, NPC^{+}). As expected, control iPSCs strongly stained for NANOG, SOX2 and OCT4 (Fig. 3.8 A, B and C). These results confirmed the stemness of the reprogrammed control iPSCs. On the other hand, in control NPCs, NANOG signal was reduced, almost non-existent, while SOX2 nuclear signal was observed, although at much lower levels than in control iPSCs (Fig. 3.8 A and B). Indeed, we were expecting to see stronger SOX2 staining than we observed. Control NPCs also presented a fluorescent signal for NESTIN expression (Fig. 3.8 C), however, this pattern of staining did not resemble the typical NESTIN-specific IF pattern noticed in NPCs from previous reports (Lyu *et al*, 2013; Quadrato *et al*, 2014). One possible control experiment would be to perform a *NESTIN* IF in iPSCs, which do not express this gene.

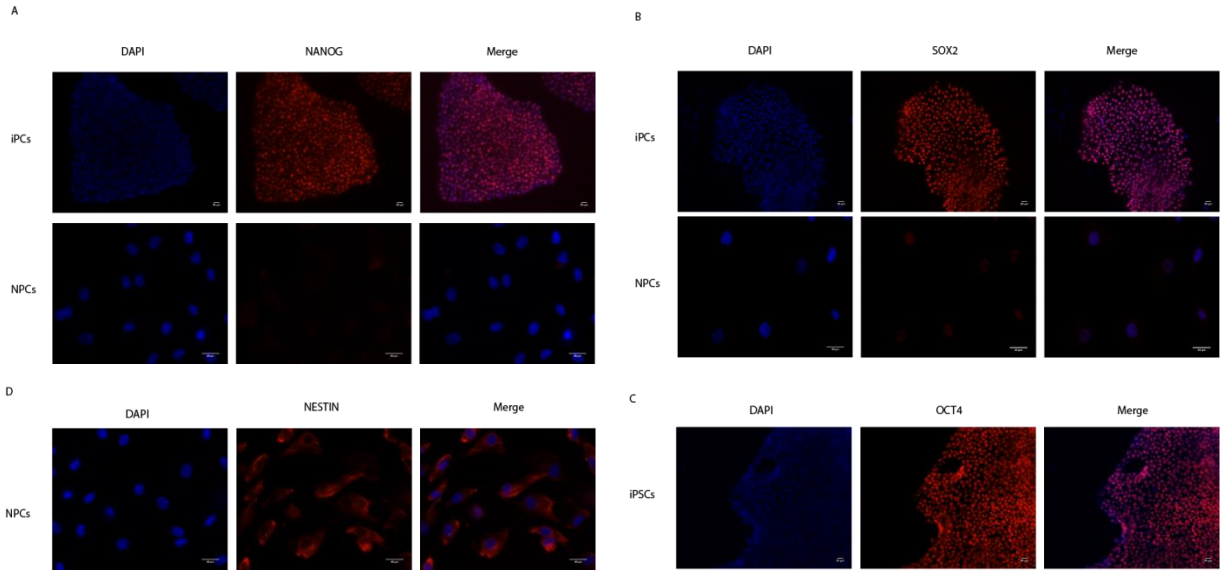

Fig. 3.8 - Representative pictures of IF assay in iPSCs and/or NPCs. A – IF assay using NANOG antibody in iPSCs and NPCs. B - IF assay using SOX2 antibody in iPSCs and NPCs. C – IF assay using OCT4 antibody in iPSCs. D – IF assay using NESTIN antibody in NPCs. Scale bar: 20μM.

Our IF results suggest that control and AS iPSCs express the expected pluripotency markers, however, for NPCs, the staining of NPC-markers was less clear. For this reason, we decided to complement this analysis with RT-qPCR to analyse the expression of the stem cell markers *SOX2*, *OCT4* and *NANOG*, the NPC-specific gene *NESTIN* and the early (*TUJ1*) and the late (*MAP2*) neuronal genes.

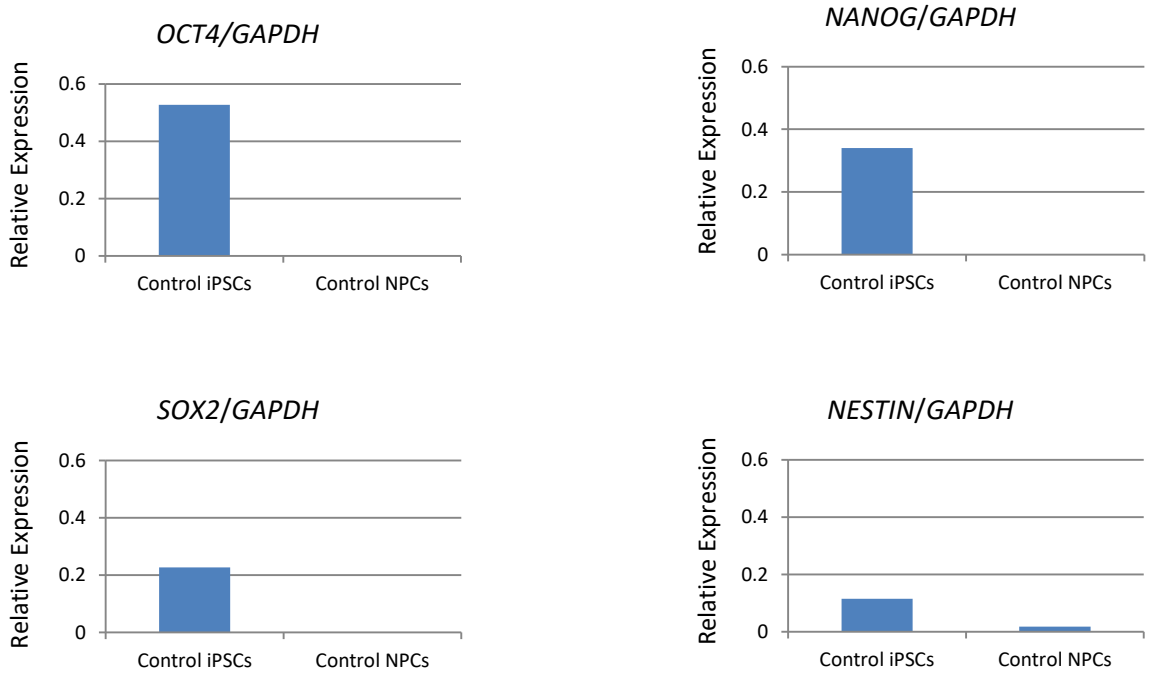

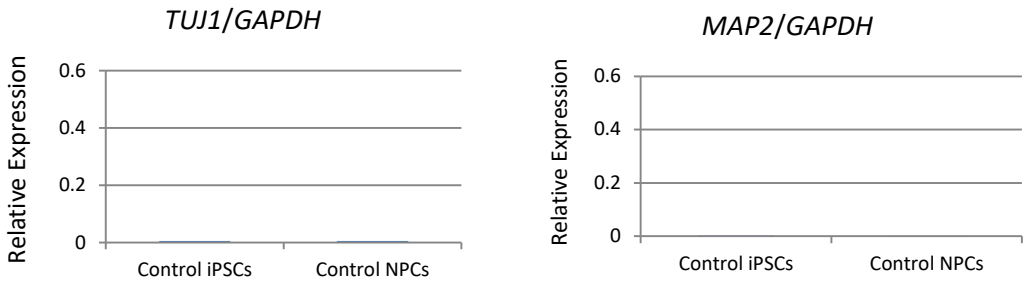

Fig. 3.9 - RT-qPCR analysis of the relative expression of the stem cells markers *OCT4*, *NANOG*, *SOX2*, the early neuronal-specific gene *TUJ1* and the late neuronal-specific gene *MAP2* in control iPSCs and control NPCs. *GAPDH* was used as a housekeeping control gene.

OCT4 and *NANOG* expression were only detectable in iPSCs (Fig.3.9) which is in line with the expected results since both of them are stem cells markers. *SOX2* expression was also only detected in iPSCs with non-considerable expression in NPCs. It would be expected a higher *SOX2* expression in NPCs than the results obtained. This goes in line with the fact that *SOX2* levels are reduced when evaluated by IF in the same cells (Fig. 3.8 B) suggesting that these cells might not be bona-fide NPCs. Moreover, *NESTIN* relative expression levels were higher in iPSCs than in NPCs (Fig. 3.9). These are unexpected results since *NESTIN* is an NPC-specific marker. Finally, we decided to evaluate both *TUJ1* and *MAP2* expression to understand whether the generated NPCs have started to exhibit signs of neuronal differentiation. Both in iPSCs and NPCs, the levels of *TUJ1* and *MAP2* were extremely low (CT mean around 30,7 and 32), respectively suggesting that the NPCs did not start acquiring a neuronal identity.

Taken together, both IF and RT-qPCR results strongly suggest that the obtained "NPCs" did not acquired a neuronal identity upon iPSCs neural differentiation. Despite following an established commercially available protocol, we were not successful at generating NPCs from iPSCs. A few aspects may have contributed to this unexpected outcome. In the STEMdiff™ monolayer protocol, as depicted in Fig. 3.7 C, upon plating iPSC single cells, passaging was expected to be performed at intervals of 6 to 9 days as induction to NPCs would slow down the division rate and cells would take longer to reach confluency. However, we observed that during NPC generation, cells were dividing at a faster rate and reaching confluency in about three days, at which point they were passaged. The higher division rate of the converting cells expedited the induction process which could have interfered with the correct induction of iPSCs into NPCs.

An interesting aspect to take into consideration is that we used newly-generated iPSCs in this study which were not differentiated into NPCs before. So far, these iPSCs have been only characterized in terms of correct expression of stem cells markers (Fig. 3.7 A, B and C) but no further assessment of pluripotency of these reprogrammed iPSCs has been tested in assays such as embryoid bodies or teratomas formation in order to prove their capacity of differentiation into the three cell lineages. At this point we cannot rule out whether the iPSCs derived from an AS patient and age-

matched and gender-matched control used in our study are able to differentiate into the neural lineages. These tests are ongoing but not finished in the scope of this thesis.

Finally, we should consider in the future generating NPCs using the STEMdiff™ embryoid bodies protocol. Despite being much more laborious and time-consuming than monolayer protocol, it is also an established and optimized protocol for generating NPCs. The embryoid bodies system enhances both cell-to-cell and cell-to-matrix interactions as well as maintains the stemness of the iPSCs (reviewed Chandrasekaran *et al*, 2016). Additionally, the use of the embryoid bodies protocol would simultaneously serve as an assessment of the iPSCs pluripotency.

3.3. Evaluation of imprinting status of genes in the Angelman locus by nascent-transcript RNA FISH

A successful and efficient differentiation into patient-derived neurons is crucial to establish an *in vitro* cellular system to study AS. Besides deriving neurons, which so far we were not successful, these neurons must exhibit the proper imprinting status for the *UBE3A* gene and other in the AS imprinted region. For this reason, we decided to test whether nascent-transcript RNA FISH would be a good tool to evaluate imprinted expression, *i. e.*, parental-specific monoallelic expression. It would be important to streamline this technique as a read-out in the future to test the effect of putative drugs in, for example, reactivation of the *UBE3A* gene. For that, we decided to focus on the expression of the *UBE3A* gene, which is biallelically expressed in most cells but only maternally expressed in neurons, and *SNORD116* gene, which is paternally expressed in all cell-types. An *UBE3A* probe had been previously generated based on Stellaris™ FISH technology (see Material and Methods) and shown to work on control and AS fibroblasts (Brandão, 2016). Stellaris™ FISH technology is an mRNA detection method that enables the detection and localization of single RNA molecules at cellular level (Orjalo *et al*, 2011). The obtained fluorescent signal is a specific signal, with a high signal-to-background ratio (Orjalo and Johansson, 2016). Besides this, the probe preparation time and complexity are reduced due to the online probe designer and their automated manufacturing (Orjalo and Johansson, 2016). For *SNORD116*, a BAC probe generated through incorporation of fluorescent d-UTP using nick translation has been previously published to work well in iPSCs (Chen *et al*, 2016). Despite the differences in the type of probes, we decided to combine the two probes in the same protocol, in order to get signal for both *UBE3A* and *SNORD116* nascent transcripts in the same cell. We tried such an approach in control and AS fibroblasts and iPSCs and also on our control "NPCs". In all the cell types, both *UBE3A* and *SNORD116* fluorescent signals were detected in the nucleus: a defined dot for the nascent *UBE3A* and a cloud-shaped signal or a less defined dot for *SNORD116*. In the control lines (fibroblasts, iPSCs and "NPCs"), we expected *SNORD116* to be imprinted and expressed only from the paternal allele, while *UBE3A*, which is only imprinted in neurons, to be biallelically expressed (Fig. 3.10 A). In AS lines, we expected only the paternal *SNORD116* and *UBE3A* to be expressed since the maternal copy of both genes are not present in these cells (Fig. 3.10 A). As expected, two *UBE3A* signals and one *SNORD116* signal could be observed in control fibroblasts, iPSCs and "NPCs", with the *SNORD116* signal co-localizing with one *UBE3A*, corresponding to the paternal allele (Fig. 3.10

B). In AS fibroblasts and AS iPSCs, one *UBE3A* signal is detected and co-localizes with one *SNORD116* signal, also corresponding to the paternal allele (Fig. 3.10 B). AS NPCs were not generated within the time of this master dissertation study and, therefore, no representative images of these cells are presented.

A

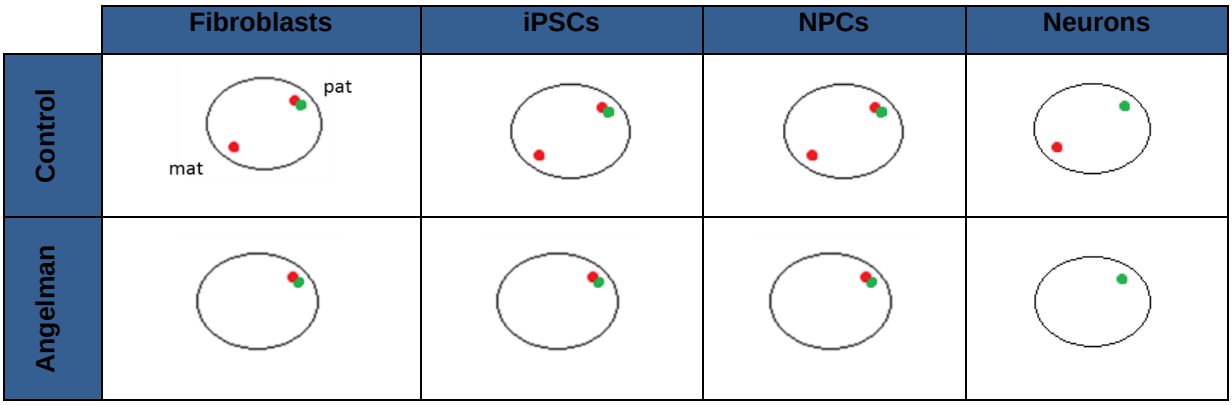

B

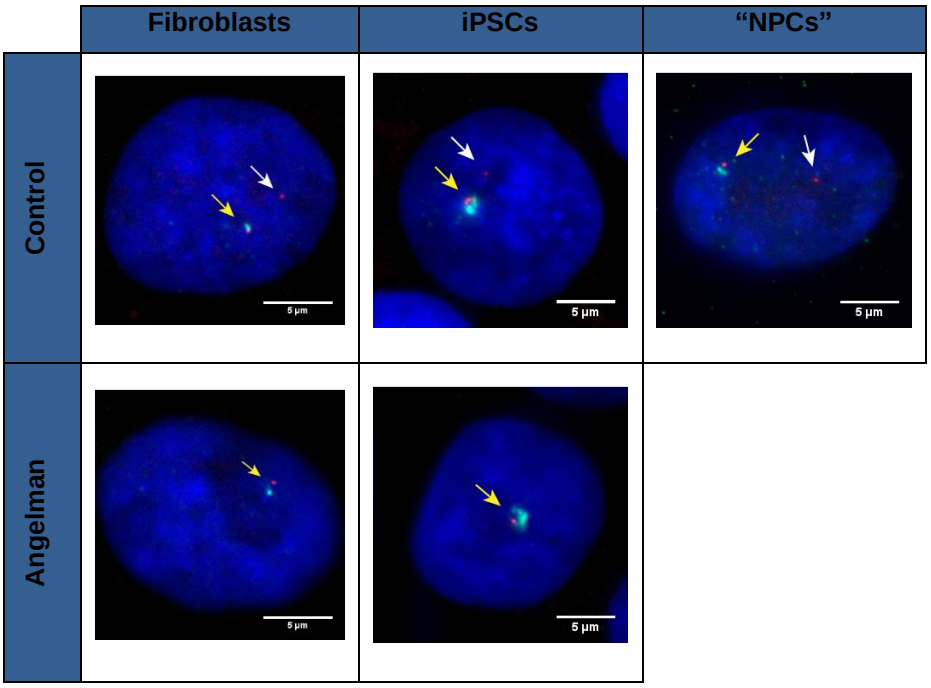

Fig. 3.10 - Expected results for *UBE3A* (red) and *SNORD116* (green) signals in fibroblasts, iPSCs, "NPCs" and neurons. A – Representative scheme of expected *UBE3A* and *SNORD116* signals in fibroblasts, iPSCs, NPCs and neurons. B - Representative images of Stellaris™ RNA-FISH assay with *UBE3A* (red) and S*NORD116* (green) probes in fibroblasts, iPSCs and "NPCs". The yellow arrows indicate the paternal allele with double signalling and the white arrows indicate de maternal allele with single signalling. Scale bar: 5µM.

These results were very encouraging since we could combine *UBE3A* and *SNORD116* probes in the same experiment, despite the differences in the type of probes. Nevertheless, despite the expected pattern being observed in several cells, other fluorescent signal patterns were also observed for all the studied cells (Table 3.1). For instance, in control fibroblasts, it was expected that the most of

the cells presented two signals for *UBE3A*, however, the percentage of 2 signals and one signal that we detected was very similar, 39% and 43%, respectively (Table 3.1). We also detected 18% of control fibroblasts with no *UBE3A* signal, which in "NPCs" is as high as 30%. In the case of AS fibroblasts, 51% of cells have the expected one *UBE3A* signal and 41% show no signal. The results seem to suggest that either the *UBE3A* alleles are not always expressed or that our method is not able to detect with 100% accuracy all *UBE3A* nascent-transcripts. Interestingly, in AS fibroblasts, 8% of cells exhibited two *UBE3A* signals (corresponding to approximately 3 cells). Since these cells have only one copy of *UBE3A*, such results might suggest that a few cells could become aneuploidy in culture or could correspond to false positive signals. Regarding *SNORD116* expression, the percentage of two signals, especially in control fibroblasts (21%), but also in AS fibroblasts (8%) (Table 3.1) was unexpectedly high. *SNORD116* is only expressed from the paternal allele in both neuronal and non-neuronal cells, whereby a single signal for this gene is the expected result. The existence of two signals for *SNORD116* can be explained by technical or counting errors. In fact, the signal of *SNORD116* in fibroblasts, which is a single dot, it is markedly different from the one in iPSCs, which is a big cloud-shaped signal. The existence of more background signal in fibroblasts RNA FISH and the less distinctive *SNORD116* signal makes the distinction between signal and background more difficult and may result sometimes in the count of two signals. In the resulting iPSCs (both control and AS), almost 100% of cells have one signal which also suggest that *SNORD116* imprinted expression should be normal in the fibroblast even if sometimes 2 signals are counted. When comparing RNA FISH results among the different cell types, we can notice that, in general, detection of both *UBE3A* and *SNORD116* signals was higher in iPSCs than in fibroblasts and "NPCs". On one hand, this could be explained by the fact that these genes are more expressed in iPSCs than in the other cell types. Another hypothesis, probably more likely, it is the fact that our RNA FISH conditions are more optimized for iPSCs than for the other cell types. It will be interesting to use, for instance, RNA FISH for a house keeping gene in these conditions to evaluate this hypothesis.

Table 3.1- Percentage of cells with two, one or no signal for *UBE3A* and *SNORD116* probes in Stellaris™ RNA-FISH in control fibroblasts, AS fibroblasts, control iPSCs, AS iPSCs and control "NPCs", and total number of each cell type counted. +/+ represents detection of gene expression in both alleles; +/- represents detection of gene expression in one allele; -/- represents no detection of gene expression.

	UBE3A			***SNORD116***			
	+/+	+/-	-/-	+/+	+/-	-/-	Total nº of cells
Control Fib	39%	43%	18%	21%	32%	47%	28 (1 slide)
AS Fib	8%	51%	41%	8%	39%	53%	39 (1 slide)
Control iPSCs	68%	30%	2%	0%	100%	0%	143 (2 slides)
AS iPSCs	1%	56%	43%	0%	97%	3%	167 (3 slides)
Control "NPCs"	25%	36%	30%	0%	40%	60%	134 (3 slides)

The percentages presented on Table 3.1 are the outcome of the mean number of cells with two, one or no signal for *UBE3A* and *SNORD116* probes in each cell type studied from several experiments. Indeed, in some cases, when comparing different experiments using the same cell line, it is possible to observe technical variations. Table 3.2 contains the counts conducted on two different

slides for AS iPSCs. It is clear that the number of cells where *UBE3A* is being detected is higher in Slide nº 2 than in Slide nº1, where many cells do not present any *UBE3A* signal. These results show that the current Stellaris™ RNA FISH conditions might not give the exact same results, even in iPSCs. This indicates that, when using this nascent-transcript RNA FISH technique, it is necessary to perform several replicates in order to obtain reliable results.

Table 3.2 - Percentage of cells with two, one or no signal for *UBE3A* and *SNORD116* probes in Stellaris™ RNA-FISH in AS iPSCs and total nº of cells counted. +/+ represents detection of gene expression in both alleles; +/- represents detection of gene expression in one allele; -/- represents no detection of gene expression.

	UBE3A			***SNORD116***			
	+/+	+/-	-/-	+/+	+/-	-/-	Total nº of cells
Slide nº1	1%	32%	67%	0%	94%	6%	72
Slide nº2	0%	81%	19%	0%	100%	0%	36

Nevertheless, we were able to optimize Stellaris™ RNA-FISH, combining a Stellaris probe (*UBE3A*) with a BAC probe (*SNORD116*) in several cell lines with three different identities: fibroblasts, iPSCs and “NPCs”. Characterization of these cells by RNA-FISH is of extreme importance because it allows monitoring of the correct imprinted expression of the Angelman locus in each differentiation stage, which is the key-aspect for the reprogrammed cells to constitute a reliable model system for Angelman Syndrome.

4. Concluding Remarks and Future Perspectives

The major aim of the project is the development of a reliable human disease modelling system to study Angelman Syndrome. We sought to generate AS patient-derived and age and gender-matched neurons either through neural direct conversion or iPSCs neural differentiation, and characterize their neuronal identity and imprinted expression of the Angelman locus.

First, we tried to perform, for the first time in our laboratory, neural direct conversion of 30 years-old and age and gender-matched patient-derived fibroblasts into induced neurons following a dox-inducible lentiviral strategy for expression of *ASCL1* and *NGN2* neural-specific transcription factor along with maintenance of the cells in a conversion medium supplemented with SMAD pathway inhibitors and then a maturation medium supplemented with neurotrophic factors. The infection efficiency of this conversion was controlled through a GFP lentiviral infection, which showed high percentage of GFP-positive cells. Control and AS 30y cells subjected to neural direct conversion were characterized by RT-PCR, RT-qPCR and IF. RT-PCR confirmed the expression of the *ASCL1* lentiviral cassette by both control and AS 30y iNs, however, RT-qPCR and IF analysis suggested that the infected fibroblasts, or at least the majority of them, did not acquired neuronal identity. In the future, when revisiting this protocol, a few aspects should be considered in order to successfully convert fibroblasts into iNs. Namely, the concentration and purification of the lentiviruses through ultracentrifugation in order to enhance the infection efficiency and the proper double antibiotic selection to guarantee that the cells subjected to neural direct conversion actually express reasonable levels of the *ASCL1-NGN2* lentiviral cassette. Furthermore, a search for either better suited enhanced neuronal-coatings and/or other coverslips than regular plastic or glass coverslips is of extreme importance since progressive dislodging of the cells under direct conversion posed as a serious problem throughout all the conversion and downstream imaging experiments.

Then, patient-derived and reprogrammed iPSCs were subjected to neural differentiation following the commercially available STEMCELL Technologies monolayer protocol into NPCs, which were also characterized by RT-qPCR and IF assays. Both assays confirmed the expression of stem cells markers by the reprogrammed iPSCs but results did not point to acquisition of a NPC bona-fide. Despite following an optimized commercial protocol, we were not successful in generating patient-derived neuronal cells. In the future, troubleshooting will be necessary. First, iPSCs, despite having the correct morphology and stem cell marker expression, should be evaluated for their pluripotent capacity through embryoid body and/or teratoma formation. Full and correct assessment of iPSCs pluripotency it is mandatory before repeating this protocol, in order to rule out any major inability of these cells to undergo neuronal differentiation. Second, it should be seriously considered the hypothesis of generating NPCs not through a monolayer protocol, but through an embryoid bodies protocol since this one presents higher conversion efficiency.

In any case, after establishing an *in vitro* cellular model system for AS it is necessary to be able to evaluate the proper imprinting expression of the Angelman locus in the generated neurons. Here, we have optimized nascent-transcript RNA FISH, combining a Stellaris and a BAC probe for, *UBE3A* and *SNORD116* expression, respectively, for three different cell-stages from fibroblast, iPSCs to

converted “NPCs”. Besides evaluating the imprinting status of Angelman-related genes, this poses a technique that can serve as a read-out for drug screening.

A human model system for AS will not only allow deepening the knowledge of the molecular aspects behind this disease but, most importantly, will serve as a platform to screen for possible putative drugs that reactivate the paternal *UBE3A* and potentially ameliorate neuronal AS-related symptoms. The establishment of such a system could give important insights for the development of therapeutic approaches for AS.

5. References

Ambasudhan, R. *et al.* (2011) 'Direct reprogramming of adult human fibroblasts to functional neurons under defined conditions', *Cell Stem Cell*, 9(2), pp. 113–118.

An, N., Xu, H., Gao, W. and Yang, H. (2016) 'Direct Conversion of Somatic Cells into Induced Neurons', *Molecular Neurobiology*, available at https://link.springer.com/article/10.1007/s12035-016-0350-0.

Angelman, H. (1965) '"Puppet" Children A Report on Three Cases', *Developmental Medicine & Child Neurology*, 7(6), pp. 681–688.

Avior, Y., Sagi, I. and Benvenisty, N. (2016) 'Pluripotent stem cells in disease modelling and drug discovery', *Nature Reviews Molecular Cell Biology*, 17(3), pp. 170–182.

Bartolomei, M. S. and Ferguson-Smith, A. C. (2011) 'Mammalian Genomic Imprinting', *Cold Spring Harbor Perspectives in Biology*, 3(7), pp. 1–17.

Bi, X. *et al.* (2016) 'Potential therapeutic approaches for Angleman Syndrome', *Expert Opinion on Therapeutic Targets*, 20(5), pp. 601–613.

Bird, L. M. (2014) 'Angelman syndrome: Review of clinical and molecular aspects', *Application of Clinical Genetics*, 7, pp. 93–104.

Brandão, D. P. (2016) 'Generation and characterization of Angelman Syndrome iPSCs for disease modelling and drug screening'. Dissertação de Mestrado. Faculdade de Ciências, Universidade do Porto.

Buiting, K., Williams, C. and Horsthemke, B. (2016) 'Angelman syndrome — insights into a rare neurogenetic disorder', *Nature Reviews Neurology*, 12(10), pp. 584–593.

Capetian, P. *et al.* (2016) 'Plasmid-Based Generation of Induced Neural Stem Cells from Adult Human Fibroblasts', *Frontiers in Cellular Neuroscience*, 10(245), pp. 3–7.

Chamberlain, S. J. (2013) 'RNAs of the human chromsome 15q11-q13 imprinted region', *Willey Interdisciplinary Reviews*, 4(2), pp. 155–166.

Chandrasekaran, A. *et al.* (2016) 'Astrocyte Differentiation of Human Pluripotent Stem Cells: New Tools for Neurological Disorder Research', *Frontiers in Cellular Neuroscience*, 10(215), pp. 1–27.

Charalambous, M., da Rocha, S. T. and Ferguson-smith, A. C. (2007) 'Genomic imprinting , growth control and the allocation of nutritional resources : consequences for postnatal life', *Current Opinion in Endocrinilogy, Diabetes & Obesity*, 14, pp. 3–12.

Chen, P.-F. *et al.* (2016) 'RBFOX1 and RBFOX2 are dispensable in iPSCs and iPSC-derived neurons and do not contribute to neural-specific paternal UBE3A silencing', *Scientific Reports*, 6(25368), pp. 1-13.

Condon K. H. et al. (2013) 'The Angelman Syndrome Protein Ube3a/E6AP is Required for Golgi Acidification and Surface Protein Sialylation', *Journal of Neuroscience*, 33(9), pp. 3799–3814.

Daily, J. L. *et al.* (2011) 'Adeno-associated virus-mediated rescue of the cognitive defects in a mouse model for Angelman syndrome', *PLoS ONE*, 6(12), pp. 1-7.

Dimos, J. T. *et al.* (2008) 'Induced Pluripotent Stem Cells Generated from Patients with ALS Can Be Differentiated into Motor Neurons', *Science*, 321(5893), pp. 1218–1221.

Dindot, S. V *et al.* (2008) 'The Angelman syndrome ubiquitin ligase localizes to the synapse and nucleus, and maternal deficiency results in abnormal dendritic spine morphology', *Human Molecular Genetics*, 17(1), pp. 111–118.

Dueñas, F. *et al.* (2014) 'Hepatogenic and neurogenic differentiation of bone marrow mesenchymal stem cells from abattoir-derived bovine fetuses', *BMC Veterinary Research*, 10(154), pp.1-13.

Egger, G. *et al.* (2004) 'Epigenetics in human disease and prospects for epigenetic therapy', *Nature*, 429(6990), pp. 457–463.

Gopalakrishnan, S., Hor, P. and Ichida, J. K. (2015) 'New approaches for direct conversion of patient fi broblasts into neural cells', *Brain Research*, 1656, pp. 2–13.

Gray, T. A., Saitoh, S. and Nicholls, R. D. (1999) 'An imprinted, mammalian bicistronic transcript encodes two independent proteins', *Proceedings of the National Academy of Sciences*, 96(10), pp. 5616–5621.

Gurdon, J. B., Elsdale, T. R. and Fischberg, M. (1958) 'Sexually Mature Individuals of Xenopus laevis from the Transplantation of Single Somatic Nuclei', *Nature*, 182, pp. 64–65.

Haase, A. *et al.* (2009) 'Generation of Induced Pluripotent Stem Cells from Human Cord Blood', *Cell Stem Cell*, 5(4), pp. 434–441.

Hiura, H. *et al.* (2013) 'Stability of genomic imprinting in human induced pluripotent stem cells', *BMC Genetics*, 14(32), pp. 1-11.

Hogart, A. *et al.* (2007) '15q11-13 GABAA receptor genes are normally biallelically expressed in brain yet are subject to epigenetic dysregulation in autism-spectrum disorders', *Human Molecular Genetics,* 16(6), pp. 691–703.

Hu, W. *et al.* (2015) 'Direct Conversion of Normal and Alzheimer ' s Disease Human Fibroblasts into Neuronal Cells by Small Molecules', *Cell Stem Cell*, 17, pp. 204-212.

Huang, H. *et al.* (2012) 'Topoisomerase inhibitors unsilence the dormant allele of Ube3a in neurons', *Nature*, 481(7380), pp. 185–189.

Imamura, K. and Inoue, H. (2012) 'Research on neurodegenerative diseases using induced pluripotent stem cells', *Psychogeriatrics*, pp. 115–119.

Jezierski, A. *et al.* (2010) 'Probing stemness and neural commitment in human amniotic fluid cells', *Stem Cell Reviews and Reports*, 6(2), pp. 199–214.

Kalish, J. M., Jiang, C. and Bartolomei, M. S. (2014) 'Epigenetics and imprinting in human disease', *International Journal of Developmental Biology*, 58, pp. 291–298.

Kalsner , L. and Chamberlain, S. J. (2015) 'Prader-Willi, Angelman, and 15q11-q13 duplication syndromes', *Pediatrics Clinic of North America*, 62(3), pp. 587-606.

Kim, J. *et al.* (2011) 'Functional integration of dopaminergic neurons directly converted from mouse fibroblast', *Cell Stem Cell*, 108(19), pp. 7838–7843.

Kim, J., Ambasudhan, R. and Ding, S. (2012) 'Direct lineage reprogramming to neural cells', *Current Opinion in Neurobiology*, 22(5), pp. 778–784.

Koch, P. *et al.* (2006) 'Transduction of human embryonic stem cells by ecotropic retroviral vectors', *Nucleic Acids Research*, 34(18), pp. 1–12.

Kwon, D. *et al.* (2017) 'Reprogramming Enhancers in Somatic Cell Nuclear Transfer, iPSC Technology, and Direct Conversion', *Stem Cell Reviews and Reports*, pp. 24–34.

Ladewig, J. *et al.* (2012) 'Small molecules enable highly efficient neuronal conversion of human fibroblasts', *Nature Methods*, 9(6), pp. 575–580.

LaSalle, J. M., Reiter, L. T. and Chamberlain, S. J. (2015) 'Epigenetic regulation of UBE3A and roles in human neurodevelopmental disorders.', *Epigenomics*, 7(7), pp. 1213–28.

Lee, G. *et al.* (2010) 'Modeling Pathogenesis and Treatment of Familial Dysautonomia using Patient Specific iPSCs', *Nature*, 461(7262), pp. 402–406.

Li, W. *et al.* (2012) 'Chemical approaches to stem cell biology and therapeutics', *Cell Stem Cell*, 13(3), pp. 270–283.

Liu, M. *et al.* (2013) 'Small Molecules Enable Neurogenin 2 to Efficiently Convert Human Fibroblasts to Cholinergic Neurons', *Nature Commun*, 4(2183), pp. 1–19.

Liu, Y. *et al.* (2012) 'Tip110 Maintains Expression of Pluripotent Factors in and Pluripotency of Human Embryonic Stem Cells', *Stem Cells and Development*, 21(6), pp. 820–833.

Lossie, C. *et al.* (2001) 'Distinct phenotypes distinguish the molecular classes of Angelman syndrome.', *Journal of medical genetics*, 38(12), pp. 834–845.

Lyu, J. *et al*. (2013) 'Protein Phosphatase 4 and Smek complex negatively regulate Par3 and promote neuronal differentiation of neural stem/ progenitor cells', *Cell Reports*, 5(3), pp. 1-13.

Mabb, A. M. *et al.* (2016) 'Topoisomerase 1 regulates gene expression in neurons through cleavage complex-dependent and -independent mechanisms', *PLoS ONE*, 11(5), pp. 1–18.

Margolis, S. S. *et al.* (2015) 'Angelman Syndrome', *Neurotherapeutics*, 12, pp. 641–650.

Mcgrath, J. and Solter, D. (1984) 'Completion of Mouse Embryogenesis Requires Both the Maternal and Paternal Genomes', *Cell*, 37, pp. 179–183.

Meng, L. *et al.* (2013) 'Truncation of Ube3a-ATS Unsilences Paternal Ube3a and Ameliorates Behavioral Defects in the Angelman Syndrome Mouse Model', *PLoS Genetics*, 9(12), pp. 1–13.

Menon, S. *et al.* (2016) 'An overview of direct somatic reprogramming: The ins and outs of iPSCs', *International Journal of Molecular Sciences*, 17(141), pp. 1–20.

Merten, O.-W., Hebben, M. and Bovolenta, C. (2016) 'Production of lentiviral vectors', *Molecular Therapy - Methods & Clinical Development*, 3, pp. 1–14.

Mertens, J. *et al.* (2016) 'Evaluating cell reprogramming, differentiation and conversion technologies in neuroscience', *Nature Reviews Neuroscience*, 17(7), pp.

Mertz, L. G. B. *et al.* (2014) 'Neurodevelopmental outcome in Angelman syndrome: Genotype-

phenotype correlations', *Research in Developmental Disabilities*. Elsevier Ltd, 35(7), pp. 1742–1747.

Meyer, S. *et al.* (2015) 'Derivation of Adult Human Fibroblasts and their Direct Conversion into Expandable Neural Progenitor Cells.', *Journal of visualized experiment* , 21(101), pp. 1–10.

Mitchell, R. R. *et al.* (2014) 'Activation of Neural Cell Fate Programs Toward Direct Conversion of Adult Human Fibroblasts into Tri-Potent Neural Progenitors Using OCT-4', *Stem Cells and Development*, 23(16), pp. 1937–1946.

Morgan, H. D. *et al.* (2005) 'Epigenetic reprogramming in mammals', *Human Molecular Genetics*, 14(1), pp. 47–58.

Murry, C. E. and Keller, G. (2008) 'Differentiation of Embryonic Stem Cells to Clinically Relevant Populations: Lessons from Embryonic Development', *Cell*, 132, pp. 661–680.

Nazor, K. L. *et al.* (2013) 'Recurrent Variations in DNA Methylation in Human Pluripotent Stem Cells and their Differentiated Derivatives', *Cell Stem Cell*, 10(5), pp. 620–634.

Nikoletopoulou, V. and Tavernarakis, N. (2012) 'Embryonic and induced pluripotent stem cell differentiation as a tool in neurobiology', *Biotechnology Journal*, 7(9), pp. 1156–1168.

Ohnuki, M. and Takahashi, K. (2015) 'Present and future challenges of induced pluripotent stem cells', *Philosophical Transactions of the Royal Society B: Biological Sciences*, 370(1680), pp. 1–8.

Orjalo, A. Jr., Johansson, H. E. and Ruth, J. L. (2011) 'Stellaris™ fluorescence in situ hybridization (FISH) probes: a powerful tool for mRNA detection', *Nature Methods*, doi: 10.1038/nmeth.f.349.

Orjalo, A. V. J. and Johansson, H. E. (2016) 'Stellaris ® RNA Fluorescence In Situ Hybridization for the Simultaneous Detection of Immature and Mature Long Noncoding RNAs in Adherent Cells', in *Long Non-Coding RNAs: Methods and Protocols*, 1402, pp. 119–134.

Pang, Z., P. *et al*. (2011) 'Induction of human neuronal cells by defined transcription factors', 476, pp. 220-224.

Park, I. *et al.* (2008) 'Disease-Specific Induced Pluripotent Stem Cells', *Cell*, 134(5), pp. 877–886.

Pfisterer, U. *et al*. (2011) 'Direct conversion of human fibroblasts to dopaminergic neurons' , *Proceedings of the National Academy of Sciences*, 108(25), pp. 10343-10348.

Pfisterer, U. *et al*. (2011) 'Efficient induction of functional neurons from adult human fibroblasts', *Cell Cycle*, 10(19), pp. 3311-3316.

Powell, W. T. *et al.* (2013) 'R-loop formation at Snord116 mediates topotecan inhibition of Ube3a-antisense and allele-specific chromatin decondensation', *Proceedings of the National Academy of Sciences*, 110(34), pp. 13938–13943.

Quadrato, G. *et al.* (2014) 'Modulation of GABAA Receptor Signaling Increases Neurogenesis and Suppresses Anxiety through NFATc4', *The Journal of Neuroscience*, 34(25), pp. 8630–8645.

Rajender, S., Avery, K. and Agarwal, A. (2011) 'Epigenetics, spermatogenesis and male infertility', *Reviews in Mutation Research*, 727, pp. 62–71.

Reik, W. and Walter, J. (2001) 'Genomic imprinting : parental influence on the genome', *Nature Reviews Genetics*, 2, pp. 21–32.

Rougeulle, C. *et al.* (1998) ‘An imprinted antisense RNA overlaps UBE3A and a second maternally expressed transcript’, *Nature Genetics*, 19(1), pp. 15–16.

Runte, M. *et al.* (2001) ‘The IC-SNURF–SNRPN transcript serves as a host for multiple small nucleolar RNA species and as an antisense RNA for UBE3A’, *Human Molecular Genetics*, 10(23), pp. 2687–2700.

Sachdeva, R., Donkers, S. J. and Kim, S. Y. (2016) ‘Angelman syndrome: A review highlighting musculoskeletal and anatomical aberrations’, *Clinical Anatomy*, 29, pp. 561–567.

Sadakierska-Chudy, A., Kostrzewa, R. M. and Filip, M. (2015) ‘A Comprehensive View of the Epigenetic Landscape Part I: DNA Methylation, Passive and Active DNA Demethylation Pathways and Histone Variants’, *Neurotoxicity Research*, 27, pp. 84–97.

Sato, M. (2017) ‘Early Origin and Evolution of the Angelman Syndrome Ubiquitin Ligase Gene Ube3a’, *Frontiers in Cellular Neuroscience*, 11(62), pp. 1–8.

Seaberg, R. M. and Van Der Kooy, D. (2003) ‘Stem and progenitor cells: The premature desertion of rigorous definitions’, *Trends in Neurosciences*, 26(3), pp. 125–131.

Silva-santos, S. *et al.* (2015) ‘Ube3a reinstatement identifies distinct treatment windows in Angelman syndrome model mice’, *The Journal of Clinical Investigation*, 125(5), pp. 2069–2076.

Soellner, L. *et al.* (2017) ‘Recent Advances in Imprinting Disorders’, *Clinical Genetics*, 91, pp. 3–13.

Sommer, C. A. *et al.* (2009) ‘Induced pluripotent stem cell generation using a single lentiviral stem cell cassette.’, *Stem cells*, 27(3), pp. 543–9.

Sommer, C. A. and Mostoslavsky, G. (2013) ‘The evolving field of induced pluripotency: Recent progress and future challenges’, *Journal of Cellular Physiology*, 228(2), pp. 267–275.

Stanurova, J. *et al.* (2016) ‘Angelman syndrome-derived neurons display late onset of paternal UBE3A silencing’, *Scientific Reports*, 6(30792), pp. 1-9.

Surani, M. A., Barton, S. C. and Norris, M. L. (1984) ‘Development of reconstituted mouse eggs suggests imprinting of the genome during gametogenesis.’, *Nature Education*, 308(5959), pp. 548–550.

Takahashi, K. *et al.* (2007) ‘Induction of Pluripotent Stem Cells from Adult Human Fibroblasts by Defined Factors’, *Cell*, 131(5), pp. 861–872.

Takahashi, K. and Yamanaka, S. (2006) ‘Induction of Pluripotent Stem Cells from Mouse Embryonic and Adult Fibroblast Cultures by Defined Factors’, *Cell*, 126(4), pp. 663–676.

Tamburini, C. and Li, M. (2017) ‘Understanding neurodevelopmental disorders using human pluripotent stem cell-derived neurons’, *Brain Pathology*, 27(4), pp. 508–517.

Tan, W. and Bird, L. M. (2016) ‘Angelman syndrome: Current and emerging therapies in 2016’, *American Journal of Medical Genetics Part C: Seminars in Medical Genetics*, 172(4), pp. 384–401.

Vadodaria, K. C. *et al.* (2016) ‘Generating human serotonergic neurons in vitro: Methodological advances’, *BioEssays*, 38(11), pp. 1123–1129.

Vierbuchen, T. *et al.* (2010) ‘Supplementary data - Direct conversion of fibroblasts to functional

neurons by defined factors.', *Nature*, 463(7284), pp. 1035–41.

Warlich, E. *et al.* (2011) 'Lentiviral Vector Design and Imaging Approaches to Visualize the Early Stages of Cellular Reprogramming', *Molecular Therapy*. Nature Publishing Group, 19(4), pp. 782–789.

Wu, H. *et al.* (2004) 'Determination of the Role of the Human RNase H1 in the Pharmacology of DNA-like Antisense Drugs', *Journal of Biological Chemistry*, 279(17), pp. 17181–17189.

Yoo, A. S. *et al.* (2011) 'MicroRNA-mediated conversion of human fibroblasts to neurons', *Nature*, 476, pp. 228–232.